Nano Research

Open Access

Review Article

Programmable bottom-up self-assembly of nanomaterials at the nanoscale and microscale

Min Ji[§] ✉, Haiyue Gong[§], Mushi Peng, Peixin Li, Xiaolin Xie, Zhaoyu Zhou, Xiaoxue Hu, and Ye Tian ✉

College of Engineering and Applied Sciences, State Key Laboratory of Analytical Chemistry for Life Science, National Laboratory of Solid State Microstructures, Jiangsu Key Laboratory of Artificial Functional Materials, Chemistry and Biomedicine Innovation Center, Nanjing University, Nanjing 210023, China

[§] *Min Ji and Haiyue Gong contributed equally to this work.*

Cite this article: *Nano Research*, **2025**, *18*, 94907174. https://doi.org/10.26599/NR.2025.94907174

ABSTRACT: Nanomaterials have long attracted extensive attention of researchers due to their various geometric shapes and unique physicochemical properties. The emerging bottom-up assembly methodology, which leverages weak interactions, provides an effective avenue to impart spatially oriented direction to nanoscale materials. DNA-mediated assembly stands out among these strategies because of the inherent specificity of the DNA materials, and has demonstrated to be an efficient means of engineering nanomaterials in a precise, hierarchical, and programmable way. The architectures constructed from the bottom up varying in basic units, dimensions, and configurations offer numerous opportunities for customizable and exotic performance in functional devices. Here, we concentrate on discussing the diversity of the bottom-up assembly reported over the past two decades with particular emphasis on DNA-mediated assembly, and highlight the structural complexity of the corresponding assemblies. Moreover, important advances achieved in properties of multidimensional assemblies constructed by nanomaterials are divided based on the categories and explored in detail. In addition, different types of nanomaterials that can serve as building blocks are also systematically reviewed here.

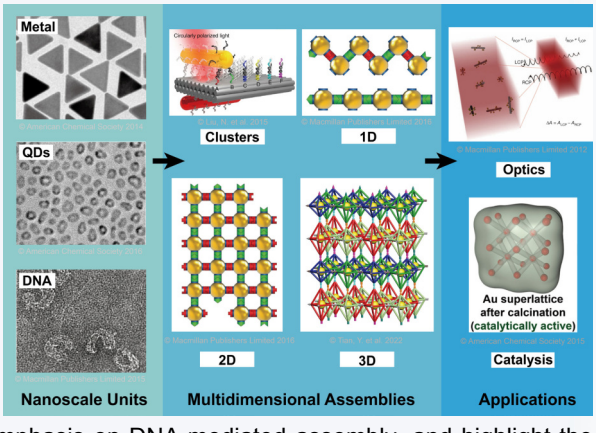

KEYWORDS: DNA nanotechnology, nanomaterials, self-assembly, programmability, bottom-up

1 Introduction

In the last century, Richard Feynman first proposed the concept of "There's plenty of room at the bottom", hinting at the possibility to assemble matter at the nanometer scale. In the subsequent decades, with significant advancements achieved in material synthesis [1–5], self-assembly [6–9], and characterization [10–12] at the nanoscale, nanotechnology has undergone exponential development leading to the emergence of numerous new materials in different dimensions.

Nanomaterials are considered as ideal candidates to serve as the fundamental building blocks in constructing high-level structures. Due to their special physical structures, numerous unique properties inherently different from bulk materials can be attained. These specific properties can be leveraged to fabricate functional devices applied in distinct scenarios. Compared with nanosized monomers, the assemblies achieved by arranging identical or different nanoparticles can have more structurally diverse configurations. Moreover, by precisely harnessing the coupling between individual components within the well-defined aggregates, these assemblies also hold significant potential for achieving highly defined properties, such as optics and catalysis [13–15]. Traditionally, the top-down methods, including lithography, etching, mechanical machining etc., are preferred for fabricating mesoscale materials with nanoscale precision. However, for nanoscale materials, the bottom-up strategies are considered a better choice due to their intrinsic molecular recognition and high adaptability to the building blocks in scale. Additionally, the bottom-up strategies can offer a series of advantages such as relaxed assembly condition, precise manipulation, and flexible programmability. In particular, precisely endowing the assembly units with highly oriented binding capabilities is crucial for

Received: September 26, 2024; **Revised:** December 4, 2024
Accepted: December 5, 2024

✉Address correspondence to Ye Tian, ytian@nju.edu.cn; Min Ji, minji@nju.edu.cn

achieving desired architectures. Ligand modification is a common and practical method, which can endow nanomaterials with adjustable weak and noncovalent interactions thereby enabling directed assembly. Among these ligands, DNA has proven to be one of the most efficient inducers for constructing superior structures because of its natural inherent properties [16–18]. Single-strand DNA is sufficient to guide nanomaterials to programmably construct multi-dimensional architectures [19], especially for three dimensional (3D) architectures. The DNA ligands modified onto the surface of nanoparticles through functional groups can bind with their complementary counterparts to realize the connection between nanoparticles. By systematically adjusting the parameters of DNA strands, a variety of highly ordered 3D architectures can be constructed varying in crystalline parameters [20, 21]. Additionally, DNA is also capable of serving as the guided materials. Due to the highly flexible programmability of DNA, a series of structurally specific DNA particles can be synthesized, including small structures composed of a few DNA strands and complex DNA origami. This ability further enriches the construction of the available architectures. Furthermore, a diverse array of nanomaterials that can be modified with DNA can be programmably positioned on the versatile platforms constructed by DNA. The periodicity present in the DNA platforms can be precisely transferred to the guest nanoparticles, creating completely new nanoparticle assemblies. To date, thousands of well-defined constructs with different configurations have been achieved, leading to various innovative properties including optics, catalysis, medicine and so on [22–24]. By finely controlling the spacing, spatial relative positions, and orientations of the nanoparticles within assemblies, we can programmably regulate the interactions between nanoparticles, enhancing the collective effect induced by the assembled architectures, which can promote the development of the fields of physics, chemistry, and material science.

In this review, we concentrate on the progress achieved in the bottom-up self-assembly over the past two decades, with a particular emphasis on DNA-mediated assembly. We begin by introducing the nanomaterials commonly used as building blocks for assembly. Then a variety of assemblies mediated by different bottom-up manners are elaborated through a series of typical cases. Subsequently, diverse properties of the assemblies are elucidated. Finally, we summarize the key points of the review and discuss the challenges and the future prospects for the bottom-up self-assembly.

2 Various types of nanoscale self-assembly motifs

Nanoscale materials are the optimal candidates to play the role as assembly motifs to construct diverse architectures. Since the initiation of systematic scientific researches on nanomaterial synthesis, tremendous types of nanoparticles have been prepared with excellent dispersibility. Common nanomaterials include metal nanoparticles, quantum dots (QDs), DNA-folded particles, and so on [25–37]. Moreover, each type of nanomaterials can be modified in terms of sizes, shapes, structures, and other characteristics to create a new series of particles, further enriching the library of assembly building blocks.

2.1 Metal nanoparticles

Metal nanoparticles generally possess excellent optical, catalytic, and magnetic properties, and thus are widely applied in various fields. Notably, these unique properties are closely related to the intrinsic geometric morphologies. Researchers systematically carried out a series of relevant researches, and have deliberately synthesized various nanoparticles with distinct shapes. Among the metal nanoparticles, the gold and silver nanoparticles (AuNPs, AgNPs) are considered as the two typical types [38–40].

As early as two thousand years ago, humans began using AuNPs in manufacturing. However, it was not until the mid-19th century that people began to consciously prepare nanoparticles. In 1951, Turkevich et al. successfully synthesized AuNPs with uniform particle sizes using citric acid to reduce chloroauric acid [41]. Until now, Turkevich method remains one of the commonly used strategies for the synthesis of AuNPs. In the initial research phase, the AuNPs obtained were still primarily spherical in shape. Nevertheless, with the rapid development of the material synthesis technology and the increasing requirement for novel properties, scientists gradually began to focus on the synthesis of non-spherical AuNPs, and successfully obtained a series of AuNPs with different shapes. In 2005, Mirkin et al. successfully synthesized triangular gold nanoplates using the seeded-mediated method [42]. However, the uniformity of the synthesized nanoplates here was not ideal, which may be caused by the uniformity of seeds that has found to be able to affect the yield of anisotropic nanoparticles. Considering these reasons, Zhang et al. proposed a seedless synthesis method using the tri-iodide ions, which inherently avoids the negative impacts brought out by seeds. By precisely adjusting the concentration of different reagents in the synthesis process, highly uniform triangular gold nanoplates can be synthesized, such as the nanoplates shown in Fig. 1(a) with a uniform edge length of 45.22 ± 3.38 nm [43]. However, seed-mediated synthesis can generally offer more advantages, such as more controllable shapes, improved monodispersity, excellent reproducibility and so on. Hence, stable acquisition of seeds with high quality is the key towards obtaining uniform AuNPs with more diverse shapes. To this end, Mirkin's group developed a strategy using iterative reductive growth and oxidative dissolution reactions to effectively adjust the quality of seeds in structures [44]. Based on a single seed source, they successfully synthesized a series of AuNPs with diverse morphologies, including cubic, concave rhombic dodecahedral, octahedral, tetrahexahedral, rhombic dodecahedral, concave cubic, cuboctahedral, and truncated ditetragonal prismatic shapes (Fig. 1(b)). The universality existing in the approach paves a way for synthesizing nanoparticles with novel morphologies, further enriching the available types of AuNPs. In addition to synthesizing from atoms, controlled overgrowth of the synthesized AuNPs is another feasible manner to achieve different shapes. By using the gold nanorods as the base, Qi and co-workers realized double arrow type AuNPs via kinetic control coupled with selective surface passivation (Fig. 1(c)) [45]. This type of AuNPs possess two pyramid-shaped ends and a four-winged axis in the middle. Moreover, through changing the concentration of $HAuCl_4$, the researchers can smoothly control the structural parameters, including the width of the ended arrows and the length of middle axis, of the double arrow type AuNPs. The tunable geometric structures allow for deliberately controlling the shift of the two plasmonic absorption peaks, effectively changing the optical properties of the nanomaterials.

The famous Lycurgus Cup was made of glass and nanomaterials including AgNPs. Compared with AuNPs with higher internal friction, AgNPs possess stronger and more durable surface plasmon resonance (SPR) signals, which results in a closer correlation

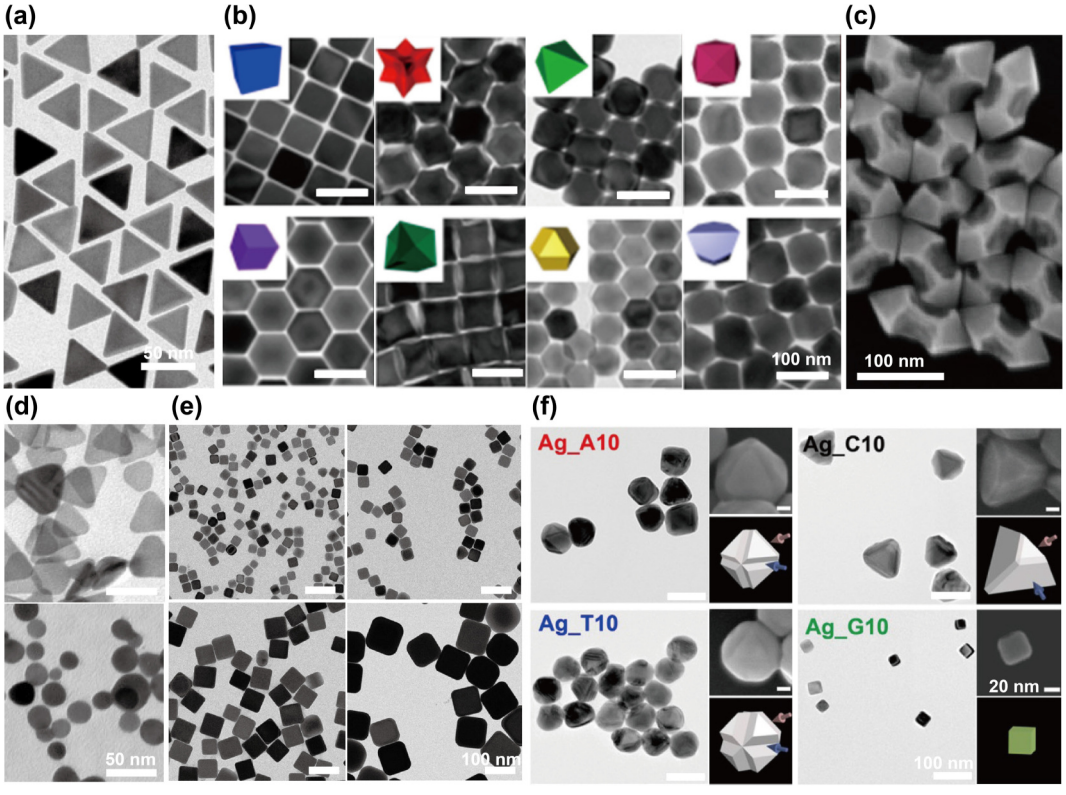

Figure 1 AuNPs and AgNPs of different shapes. (a) Triangular gold nanoplates. Reproduced with permission from Ref. [43], © American Chemical Society 2014. (b) From left to right, top to bottom: cubic, concave rhombic dodecahedral, octahedral, tetrahexahedral, rhombic dodecahedral, concave cubic, cuboctahedral, and truncated ditetragonal prismatic AuNPs. Reproduced with permission from Ref. [44], © American Chemical Society 2014. (c) Double arrow type AuNPs. Reproduced with permission from Ref. [45], © Qi, L. M. et al. 2017. (d) Triangular (top) and circular (bottom) silver nanoplates. Reproduced with permission from Ref. [46], © Wiley-VCH Verlag GmbH & Co. KGaA, Weinheim 2009. (e) Silver nanocubes with different side lengths. Reproduced with permission from Ref. [48], © American Chemical Society 2010. (f) Changing the morphologies of AgNPs by using different DNA sequences. Reproduced with permission from Ref. [49], © American Chemical Society 2014.

between the properties and morphologies of AgNPs. Hence, synthesizing AgNPs with various shapes is also considered an important research direction, and numerous researches have been systematically conducted [2]. Constantly, scientists expect to quickly stop the synthesis process of nanomaterials at a specific phase, and harvest the intermediate nanoparticles. However, it is usually difficult to completely terminate the reaction, and the intermediate products are chemically unstable. Hence, Yin et al. innovatively proposed an inverted strategy [46], in which the synthesized triangular silver nanoplates are used as the precursors (Fig. 1(d), top). Under the exposure of ultraviolet (UV) irradiation, the sharp angles of the triangles gradually become blunt, and the shapes can be transformed into circles after 125 min (Fig. 1(d), bottom). Additionally, protected by the poly(vinylpyrrolidone) (PVP), circular silver nanoplates can be stored for more than 120 days. Except for the flake-like shapes, AgNPs can also be prepared into various polyhedral shapes. In 2002, Xia et al. first successfully realized large-scale synthesis of silver nanocubes, strongly demonstrating the feasibility of synthesizing AgNPs with controllable structural parameters via chemical means [47]. Meanwhile, the achieved silver nanocubes can act as sacrificial templates to realize hollow gold nanocages. Furthermore, Xia et al. provided a seed-mediated strategy that allowed for controllably synthesizing a series of uniform silver nanocubes with side lengths from 30–200 nm, in which the single-crystal silver seeds is the key [48]. By precisely adjusting the amount of silver seeds, reaction time, and the precursor $AgNO_3$, uniform nanocubes with specific sizes can be synthesized. For example, under the condition of certain amount of silver seeds (50 μL, ~ 1.8 nM) and $AgNO_3$ (75 μL, 282 mM), silver nanocubes can exhibit a gradual increase in edge lengths with increasing reaction time (Fig. 1(e); from left to right, top to bottom: 20 min, 40 min, 2 h and 3 h). After 20 min, silver nanocubes were formed with the shortest edge length of 35 nm, while after 3 h, the nanocubes reached their maximum edge length of 97 nm. Like the PVP mentioned above, nucleic acids can serve as capping agents controlling ultimate geometric shapes of AgNPs. Distinguished from other capping agents, DNA can possess excellent programmability by encoding the strands, including the sequence and number of bases. Based on the cubic silver seeds of ~ 40 nm, Lu and his co-workers systematically explored how the single-stranded DNA impacts the geometric structures of AgNPs [49]. Four different single DNA strands composed of 10-nt A/T/C/G were selected as experimental objects, and correspondingly named as A10/T10/C10/G10. DNA-modified cubic silver seeds were mixed with L-ascorbic acid and silver acetate, and then incubated for 3 h. Due to the varying binding affinities of these DNA strands to the cubes, the seeds were selectively transformed into specific morphologies. For DNA strands A10 and T10, the shapes of AgNPs were changed to truncated stellated octahedral shapes (Fig. 1(f), left). While for C10 and G10, the resulting morphologies of AgNPs were truncated tetrahedron and cube, respectively (Fig. 1(f), right). This DNA sequence-dependent nanoparticle synthesis strategy allows for generating AgNPs with stable biorecognition capabilities, and dramatically improves the control ability to shape microscopic morphology. With the rapid development of nanomaterial synthesis, many tedious and repetitive tasks are considered more

robot-friendly. Additionally, it can reduce the workload of researchers and facilitate industrial advancement. In 2024, Han et al. developed an autonomous experimental platform for synthesizing tailorable nanoparticles, and successfully completed the preparation of desired AgNPs. These advances achieved in intelligent platform pave a way for industrially achieving more various nanoparticles [50].

2.2 Quantum dots

In 1993, Bawendi's group first successfully prepared almost monodisperse CdS, CdSe, and CdTe QDs of uniform sizes [51], marking the beginning of the controllable synthesis technology of QDs [52–54]. Similar to metal nanoparticles, shape-controllable synthesis is also of important interest in the field of QDs. The reactive temperature in the synthesis process is crucial to realize QDs with specific shapes, as it can extensively impact the dynamics of capping ligands. By precisely adjusting the temperature in the synthesis process of QDs, Li and his co-workers achieved spherical, cubic, tetragonal, and branched QDs (Fig. 2(a), from top to bottom, left to right) respectively at 260, 275, 250, and 240 °C [55]. In addition to the solid structures, researchers can also realize synthesizing QDs with hollow shapes. In 2016, Talapin et al. deliberately added Se powder to the solution of atomic precision colloidal CdSe nanoplatelets, followed by heating and cooling, and ultimately realized the synthesis of uniform CdSe nanorings (Fig. 2(b)) [56]. However, it is not until adding $Cd(HCOO)_2$ powder to the solution that CdSe nanorings can exhibit strong photoluminescence. The successful preparation of nanorings demonstrates the feasibility of producing QDs with complex topologies and represents a significant advancement in synthesis technology. At the same time, the exotic structures provide a new way to create innovative properties.

Compared with common II-VI semiconductor QDs, carbon QDs possess low toxicity, good biocompatibility, excellent optical properties, and other advantages. However, it is difficult to precisely adjust the emission wavelength of carbon QDs by altering their sizes. Most carbon QDs are only capable of emitting blue, green, and yellow light. To solve this problem, Wu's group provided an acid reagent engineering strategy utilizing o-phenylenediamine (oPD) as the precursor (Fig. 2(c)) [57]. To minimize the structural defects and excessive carbonization caused by strong acids, a series of mild acids, including folic acid, boric acid, acetic acid, and others, are separately added to oPD at specific ratios during the synthesis process. Under this strategy, researchers realized the synthesis of full-color fluorescent QDs, of which the emission ranges from blue to white light. The progress achieved in this work highlights the potential for producing carbon QDs with well-defined optical properties across a broad spectrum, and offers a new path for realizing advanced optical devices.

2.3 Proteins

Proteins are considered significant nanoscale assembly units because they can participate in numerous biological activities including metabolic processes, biological signal transduction, and so on [58]. The universality and significance of proteins in nature can be observed across bacteria, viruses, and all eukaryotic organisms with life [59]. The process of protein self-assembly is critical to realize different biological functions, as the structures resulting from protein self-assembly can provide cellular protection and enhance molecular movement. Protein assembly can serve as the basis for protein collaboration to complete life activities [60–62]. Therefore, it is significant to deeply understand the structure of proteins to facilitate the subsequent assembly.

Chen's group reported a programmable strategy to generate structures with different dimensions using the protein LecA [63]. The structure of the protein LecA is like a flat cuboid, and the inducing small-molecule ligands can be precisely modified on the four corners to realize desired architectures. Moreover, they demonstrated that the trivial structure change of the ligands is the crucial elements to assembly the native LecA into different structures using molecular simulation. Additionally, the pili filaments on the surface of many bacteria are also effective biomaterials to realize assembly of desired structures. The pili filaments are structurally long and thin similar to the wires in daily life. Isaac's group successfully realized the assemblies with high conductivity utilizing the pili filaments of a *E. coli* strain [64]. Transmission electron microscopy (TEM) images of a *E. coli* strain and pili filaments are shown in Fig. 3(a). In the assemblies, the long axis directions of the pili were kept parallel (Fig. 3(b)). Compared with the disordered pili networks, the conductivity of the ordered

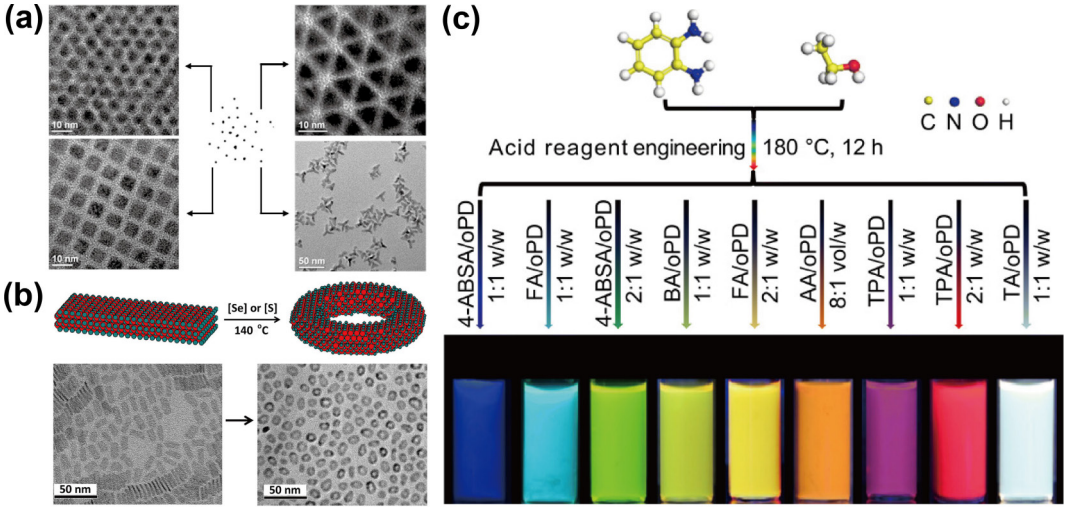

Figure 2 Various types of QDs. (a) CdSe QDs of different shapes. Reproduced with permission from Ref. [55], © American Chemical Society 2009. (b) The process of transforming CdSe nanoplatelets into CdSe nanorings. Reproduced with permission from Ref. [56], © American Chemical Society 2016. (c) The process to synthesize full-color fluorescent carbon QDs using an acid reagent engineering strategy. Reproduced with permission from Ref. [57], © Wang, L. et al. 2020.

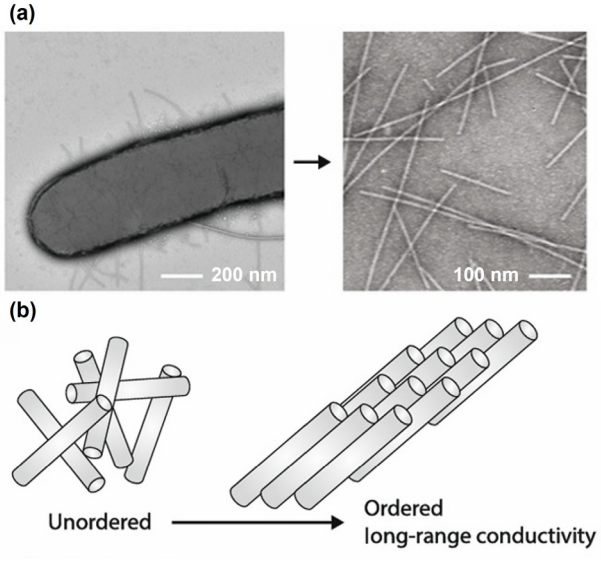

Figure 3 Assembling the pili filaments of *E. coli* strains. (a) TEM images of a *E. coli* strain (left) and pili filaments (right). (b) Assembling pili filaments into ordered structures with long-range conductivity. Reproduced with permission from Ref. [64], © Isaacs F. J. et al. 2022.

assemblies can increase 5-fold. Isaac's group experimentally realized the production of functional biomaterials using bacterial nanowires, paving the way for further applications within related electronic device sectors.

In addition, proteins can also possess irregular geometric shapes. Jerala et al. proposed a novel protein assembly strategy based on modular architectures of assembly modules that are structurally and covalently pre-organized [65, 66]. A set of peptides forming helix-helix dimers (orthogonal set) can be adapted to design protein structures, which are called coiled-coil protein origami (CCPO). CCPO is similar to DNA origami in that its design relies on the specific interactions between assembly units to promote cyclization, achieving higher stability and greater conformational homogeneity to reduce the conformational entropy of the unfolded state, thereby facilitating assembly. In the reports, protein nanostructures with shapes of tetragonal and bipyramid have been successfully generated, greatly enriching the geometric shapes of the available proteins.

2.4 DNA monomers

In 1953, Watson and Crick revolutionarily raised the DNA double helix structure model [67], revealing the base-pairing principle and the potential programmability inherently existing in the DNA [68–70]. Furthermore, the discovery of Holliday model, naturally occurring in organisms, showcases the diversity and flexibility of DNA structures, and inspired researchers to build nanostructures using DNA. In the initial phase of DNA nanotechnology, professor Seeman of New York University led his team creatively synthesized various multi-arm DNA monomers by mimicking the Holliday junction [71–74]. Subsequently, researchers uniformly named this type of structures formed by several simple DNA strands "DNA tile". Additionally, by introducing the sticky ends (SEs), Seeman's group indirectly demonstrated the potential for further assembling DNA tiles into high-dimensional structures using three-arm DNA junctions.

However, the rigidity of the DNA tile is insufficient to achieve ideal assemblies as each arm consists of only a single double-stranded DNA helix. Naturally, researchers considered to address this problem by increasing the thickness of arms. Following this intuitive but reasonable idea, Yan et al. redesigned four-arm DNA branched junction by increasing the number of double-stranded DNA helices in each arm, and the new structure was called "4 × 4 tile" [75]. After experimental characterization, 4 × 4 tile was proved to be sufficiently stable. Subsequently, researchers successfully fabricated hundred-nanometer scale 2D planes via 4 × 4 tile. It is worth mentioning that the DNA sequences used in 4 × 4 tile are asymmetric, which visibly increases the difficulty in subsequent assembly. In 2005, Mao and his co-workers optimized the design of 4 × 4 tile by simplifying the sequences of DNA into three types (Fig. 4(a)) [76]. This four-arm DNA tile via the strategy of sequence symmetry was characterized as accurately assembled and stable, and experimentally demonstrated to readily construct hundred-micron-level 2D structures. To facilitate the distinction, the new structure is called four-point-star motif. Subsequently, Mao's group have conducted targeted researches and expansions on this type of symmetric DNA tiles, and successfully constructed three-point-star [77] and six-point-star monomers [78] (Figs. 4(b) and 4(c)). Additionally, researchers can also alter the base number between adjacent DNA arms to design distinct tiles. In 2019, Wei et al. successfully designed the X-shaped DNA tile by adding DNA double strands to the connection point of the DNA arm, in which opposing DNA arms are parallel but not in a straight line [79]. Just by simply fine-tuning the structural parameters, a wide variety of DNA tiles can be readily created. Furthermore, Zhang et al. creatively proposed a novel DNA tile design idea, in which antiparallel crossover structures are combined with T-shaped structures to realize novel tiles. Under this strategy, by programmably integrating the two structures, various T-shaped crossover DNA tiles with different layers can be realized (Fig. 4(e)) [80]. In addition, by selectively adjusting the length of the horizontal and bottom horizontal arms, T-shaped crossover DNA tiles can be used to controllably create well-defined nanorings. This structurally flexible DNA tile provides a new approach to building complex high-dimensional structures.

Compared with simple and nimble DNA tile, DNA origami containing tens of thousands of bases offers a complementary manner to create DNA monomer structures. In 2006, Rothemund formally reported DNA origami technology, in which hundreds of DNA chains, called staples, can be manipulated to precisely fold a DNA main chain, called scaffold, to achieve a pre-designed structure (Fig. 5(a)) [81]. In the report, Rothemund successfully designed and synthesized diverse 2D hundred-nanometer monomer DNA origami, including square, star, smile shape, and others. These advances achieved in the monomer sizes and shapes expand application scenarios for DNA nanostructures. In the subsequent decade, researchers have conducted extensive researches on the geometric shapes of DNA origami, especially 3D structures. In 2009, Shih and his co-workers proposed a general strategy to programmably build 3D monomeric DNA origami structures [82]. Each DNA origami was designed based on the honeycomb lattice, which can effectively avoid electrostatic repulsion between DNA helices while maintaining origami rigid and stable. Various types of 3D monomer structures were designed with well-defined geometric shapes, including square nut, slotted cross, stacked cross, and so on. Additionally, Shih's group further realized twisted and curved 3D DNA origami, breaking through the conventional notion that DNA double helices are always straight [83]. Because each double helix

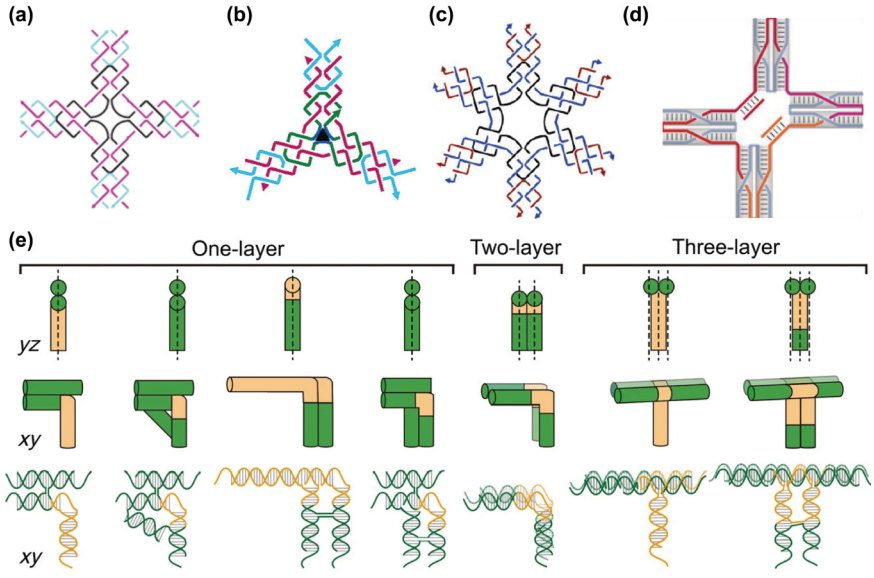

Figure 4 Diverse DNA tiles. (a) Four-point-star motif. Reproduced with permission from Ref. [76], © Wiley-VCH Verlag GmbH & Co. KGaA, Weinheim 2005. (b) Three-point-star motif. Reproduced with permission from Ref. [77], © American Chemical Society 2005. (c) Six-point-star motif. Reproduced with permission from Ref. [78], © American Chemical Society 2006. (d) X-shaped DNA tile. Reproduced with permission from Ref. [79], © Wiley-VCH Verlag GmbH & Co. KGaA, Weinheim 2019. (e) T-shaped crossover DNA tiles. Reproduced with permission from Ref. [80], © Zhang, F. et al. 2023.

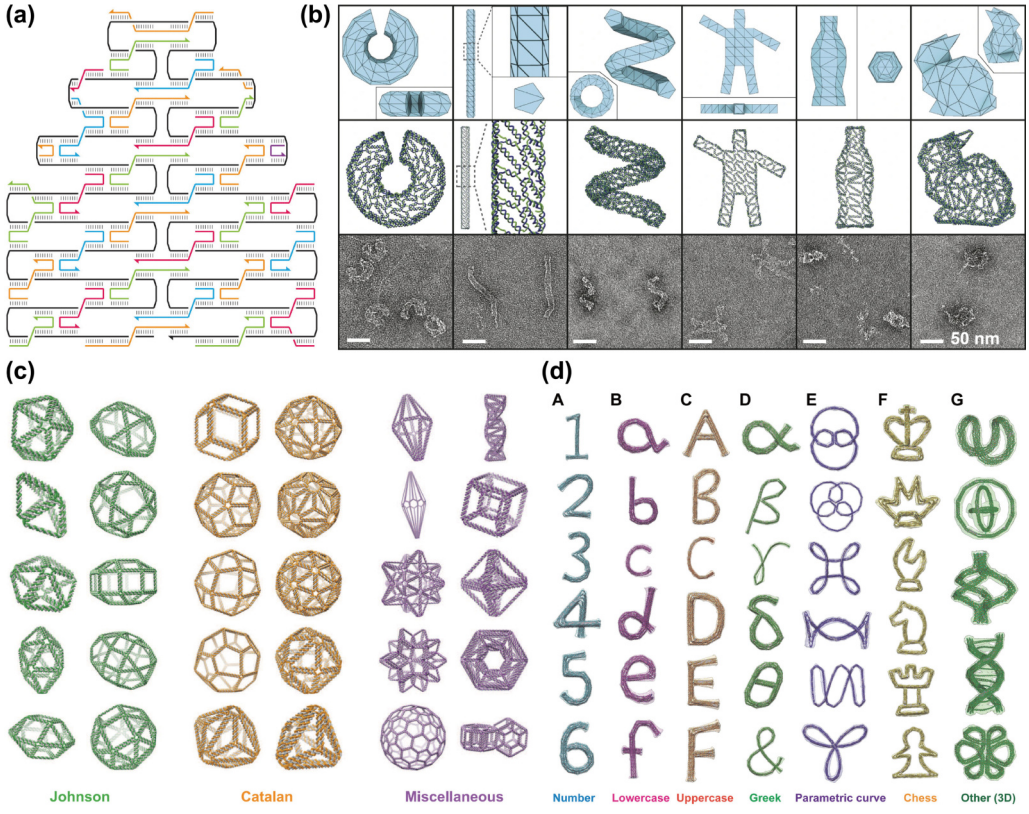

Figure 5 The excellent programmability of DNA origami. (a) 2D DNA origami. Reproduced with permission from Ref. [81], © Macmillan Publishers Limited 2006. (b) Different mesh-type DNA origami (from left to right): a nicked torus, a rod, a helix, a human, a bottle, and a rabbit. Reproduced with permission from Ref. [85], © Macmillan Publishers Limited 2015. (c) Various types of polyhedral DNA origami. Reproduced with permission from Ref. [87], © The American Association for the Advancement of Science 2016. (d) Diverse free-form DNA nanostructures. Reproduced with permission from Ref. [88], © Castro, C. E. et al. 2023.

DNA strand is physically constrained to each other, carefully controlling the number of base pairs deleted can lead to a certain degree of overwinding in the DNA segment, resulting in DNA origami twisting and curving. Similarly, Yan et al. successfully synthesized diverse intricated DNA origami with high curvature, such as the sphere, ellipsoid, and nanoflask, by bending DNA double helices, further expanding the complexity and designability of DNA origami [84]. In 2015, Högberg's group provided a general strategy to construct DNA nanostructures by using polygonal digital meshes [85]. This approach exquisitely divides the

continuous surface of the desired structures into numerous interconnected regions, enabling smooth transitions across curved surfaces and significantly reducing the complexity of folding. In this work, diverse DNA origami were experimentally demonstrated to be precisely folded, such as the helix, the human, the rabbit, and others, which are difficult to realize using other methods (Fig. 5(b)). While scientists continuously strive to create more complex origami structures, they also aim to develop smarter strategies to lower the complexity of design [86]. Bathe and his co-workers creatively proposed an algorithm that can automatically complete the design of polyhedral DNA origami by rendering desired structures as node-edge networks using DNA double crossovers. Various polyhedral DNA origami structures, including Johnson solids, Catalan solids, and miscellaneous solids, have been demonstrated to be precisely synthesized by cryo-electron microscopy (cryoEM) (Fig. 5(c)) [87]. The ability to intelligently realize DNA origami from the top bottom enables the broader application of DNA origami. Coincidentally, Castro's group introduced the user-friendly software MagicDNA 2.0 enabling the automatic design and simulation of free-form DNA origami, and they have accurately synthesized a series of DNA structures, including numbers, parametric curves, chesses, and others (Fig. 5(d)) [88]. The amazing progress achieved in structure design further enriches the library of DNA monomers and paves a way for high-dimensional DNA assemblies.

3 Controlling nanomaterials to form multidimensional assemblies

In the bottom-up self-assembly, interactions and inducing ligands are recognized as two critical elements for successfully constructing assemblies. Common weak interactions contain hydrogen bonds, electrostatic forces, van der Waals forces, etc., while inducing ligands encompass polymers, DNA, small molecules etc. In the subsequent sections, we focus our discussion on the electrostatic interaction-, polymer-, and DNA-mediated assembly. It is important to emphasize that although DNA is classified as a polymer in principle, we prefer to discuss DNA-guided assembly separately due to its unique designability and programmability.

3.1 Charged ligand-mediated self-assembly

Electrostatic interactions are typically employed to guide the assembly of nanomaterials into supramolecular structures. Objects with opposite charges can readily connect forming specific architectures. Additionally, assemblies driven by electrostatic interactions offer advantages of simplicity, reversibility, strong adaptability and so on.

Thayumanavan et al. provided a straightforward but robust strategy to programmably realize the nanostructures by introducing electrostatic interactions to the free polymers, which is inspired by the phenomenon that the electrostatic complexation can effectively impact the self-assembly [89]. Although unconventional, this approach intuitively highlights the flexibility of electrostatic interactions. In experiments, Thayumanavan's group utilized two types of polymers to carry on assembly. Each unit of these polymers consists of a hydrophilic segment and a crosslinkable segment with weak hydrophobicity. By introducing electrostatic interactions, the packing characteristics were temporarily disturbed, allowing the occurrence of the cross-linking reaction to produce a vesicle-like structure. Additionally, this type of nanoassembly can be conveniently modified to achieve functional surfaces for further applications, offering new possibilities for drug delivering, sensing, and so on.

Electrostatic interactions can also direct nanoparticles to form specific 3D superlattices. Grzybowski's group utilized AgNPs (~ 4.8 nm) and AuNPs (~ 5.1 nm) successfully constructing 3D superlattices (Fig. 6(a), top) [90]. The AgNPs and AuNPs were respectively modified with $HS(CH_2)_{10}COOH$ (MUA) and $HS(CH_2)_{11}NMe_3^+Cl^-$ (TMA) to make them positively and negatively charged (Fig. 6(a), bottom). After modification, the size of the two types of nanoparticles became more similar. The AgNPs and AuNPs were first mixed equally to produce precipitates, which were then placed in solution to generate 3D superlattices by slowly evaporating at 70 °C. The resulting nanoparticle superlattices were demonstrated to possess the sphalerite structures rather than the more tightly packed NaCl or CsCl structures (Fig. 6(b)). Additionally, researchers found that the polydispersity of the nanoparticles can remarkably impact the superlattice quality. The crystals formed from narrowly distributed nanoparticles tend to be amorphous aggregates (Fig. 6(c), left), while using the narrowly distributed AuNPs and polydisperse AgNPs, crystals can form with regular shapes (Fig. 6(c), right). Yin et al. demonstrated that continuous electrostatic interactions between silica spherical nanoparticles can be effectively established by acid treatment, and thus silica nanoparticles can be guided to form colloidal crystals of

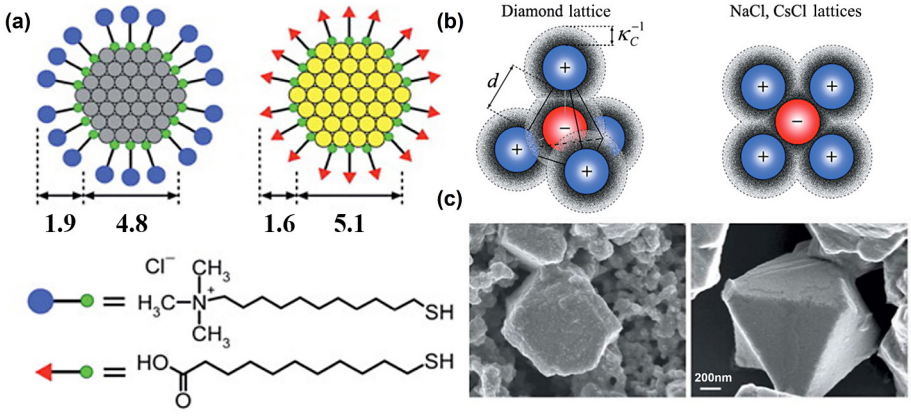

Figure 6 Assembling nanoparticles into 3D superlattices using electrostatic interactions. (a) AgNPs (top-left) and AuNPs (top-right) both modified with ligands (bottom). (b) Two types of packing modes. (c) SEM images of the nanoparticle superlattices composed of nanoparticles having different polydispersity. Reproduced with permission from Ref. [90], © The American Association for the Advancement of Science 2006.

body-centered cubic (BCC) structures [91]. These advances facilitate the fabrication of colloidal silica-based functional devices. Klajn et al. provided a robust strategy to effectively guide nanoparticles to form 3D colloidal crystals using small molecules only with three electric charges [92]. Particularly, they explored the electrostatic interactions across different scales, the molecular scale and the nano scale, and demonstrated that the small molecules with charges ≥ 3 have unique effects on assembly. These findings can offer critical insights to reveal the crystallization mechanisms. Additionally, negatively charged DNA structures can serve as the building blocks in the electrostatic force-mediated assembly. In 2015 and 2017, Dietz's group delicately designed a series of dynamic DNA structures, which can be directed to self-assemble under the influence of magnesium salt [93, 94]. The design of DNA structures mimicked the shape recognition between RNase P and tRNA. Convex and concave areas were deliberately designed to serve as the acceptor stems and the binding pockets, which ensured the shape complementarity for the assembly of DNA monomers. Notably, they designed a nanorobot composed of three distinct configurations. With the concentration of Mg^{2+} in solution increasing from 5 to 30 mM, the nanorobot will undergo three states, from dispersed to robots with arms outstretched to robots with arms closed. The successful fabrication of dynamic robots offers more opportunities to create nanoscale dynamic devices.

3.2 Polymer-mediated self-assembly

Polymer-mediated assembly has been widely demonstrated to be a useful approach for guiding nanomaterials to construct well-defined structures in a controllable manner. Polymers can readily promote the integration of nanoparticles into various architectures, typically realized by modifying polymers on the surface of nanoparticles. During the process of assembly, it is essential to avoid too strong interactions, as they can result in disordered assemblies composed of local structures with minima energy. Additionally, diverse weak interactions can be utilized in the polymer-mediated assembly, including electrostatic forces [90], hydrogen bonds [95], hydrophilic and hydrophobic interactions [96], etc. These diverse accessible interactions facilitate the application of polymer-mediated strategies across different scenarios.

Poly(ethylene glycol) (PEG) is one of the common polymers utilized to construct architectures. Caruso's group described a strategy to generate PEG particles employing the mesoporous silica (MS) as templates (Fig. 7(a)) [97]. They delicately infiltrated different types of PEG units into spherical MS (MS@PEG), and successfully produced four kinds of PEG particles by removing the MS core. Each arm of the PEG building blocks are identical, with the number of the arms being the only variable. With the number of arms increasing, the molecular weights of both the PEG building blocks and resulting PEG particles increase. The self-assembling capability of the polymers lays the foundation for obtaining a wider variety of assemblies. Furthermore, Caruso's group provided a one-pot strategy to synthesize functional nanoparticles in solution by introducing the polymers [98]. PEG was also selected to play the role as polymers. In this report, Caruso's group successfully constructed a series of bioactive nanoparticles by utilizing PEG, biomacromolecules, metal ions, and polyphenols (Fig. 7(b)).

Typically, polymers act as the inducing ligands during the assembly. Sun and colleagues reported a layer-by-layer method to guide magnetic nanoparticles in forming smooth magnetic films [99]. During the assembly process, different polymers, including the poly(vinylpyrrolidone) (PVP) and poly(ethylenimine) (PEI), were used to take place of the oleic acid or oleylamine near the Fe-Pt nanoparticles to facilitate the controllable assembly. Both dimensions and thickness of the structures fabricated here are able to be precisely adjusted. The strategy can be applied to other substrates with different sizes and configurations. Similarly, Müller-Buschbaum et al. described a polymer-mediated route based on the place-exchange reaction to construct multi-dimensional networks composed of Fe-Pt nanoparticles, and two types of nanoparticle arrangements can be found from the ultimate products, the cubic and hexagonal close packing structures [100]. Moreover, hydrogen bonds can also be applied in the polymer-guided assembly. In 2021, Macfarlane's group provided a robust method to construct macroscopic materials using nanoparticles modified with polymer chains [101]. Each polymer chain ends with a supramolecular group that enables the connections between nanoparticles via hydrogen bonding forces. By heating and stressing the pre-synthesized micron-sized crystals, millimeter-scale crystals can be readily fabricated without losing the crystallinity, which is attributed to the dynamic hydrogen bonding interactions between adjacent nanoparticles. Furthermore, Macfarlane's group systematically investigated the crystallization of nanoparticles and multivalent polymers via hydrogen bonds [95]. Their studies explored various factors, including the size and shape of multivalent scaffolds, enabling the fabrication of high-quality devices with precise control.

3.3 DNA-mediated self-assembly

In 1982, Seeman, a pioneer in DNA nanotechnology, creatively purposed that DNA can serve as material components to build a

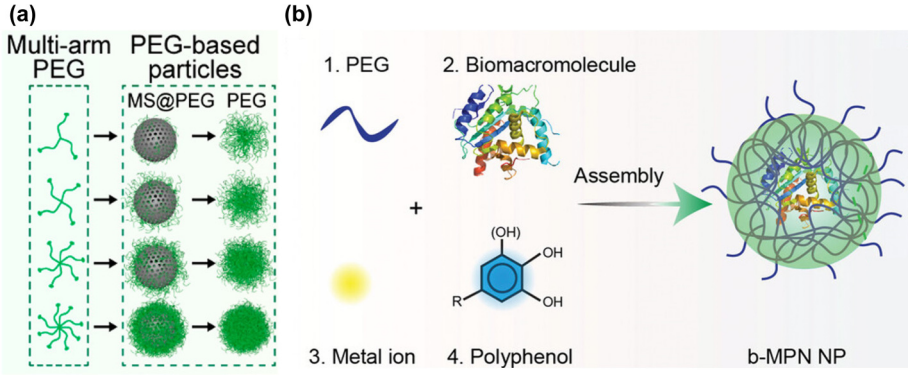

Figure 7 Different polymer-mediated structures. (a) Using different types of PEG units to generate MS@PEG and PEG nanoparticles. Reproduced with permission from Ref. [97], © American Chemical Society 2021. (b) The process to form b-MPN nanoparticles. Reproduced with permission from Ref. [98], © Wiley-VCH Verlag GmbH 2022.

diversity of multi-dimensional structures [71]. Since then, the prelude of DNA nanotechnology has officially begun, and with the rise of nanotechnology in the 1990s, DNA nanotechnology began to advance rapidly. Watson–Crick base-pairing principle is one of the most representative characteristics of DNA materials, which allows for encoding DNA strands using specific bases. As a result, an extremely diverse range of DNA strands can be generated, differing in sequences and lengths, leading to numerous hybridization interactions that remain mutually independent throughout the assembly process. Additionally, profound molecular biology research has shown that the double helix structures present in DNA have stable and fixed structural parameters. For B-type DNA, the most prevalent form found in cells, the helical radius and period are ~ 2 and ~ 3.4 nm, respectively. These precise structural parameters facilitate the programmable design and accurate predication of DNA-mediated assemblies, effectively increasing the scalability of the achieved multi-dimensional structures.

3.3.1 Based on simple DNA structures

When studying the motion of DNA, Seeman recognized that the asymmetric synthetic DNA strands have the potential to form branched structures with immobile branched points. Additionally, these branched structures can interconnect with each other by extending additional DNA sequences, which are not incorporated in the branched structures. It was not until 1982 that Seeman reported a complete vision for DNA nanotechnology, and pointed out the original purpose of DNA mediated self-assembly [71]. Additionally, Seeman provided a preliminary but meticulous method to construct 3D DNA structures. First, researchers should complete the design and preparation of DNA monomers with assembly ability. Then, the 3D structures can be assembled through the interconnection between the synthesized DNA monomers. Therefore, the specificity, directionality, and number of the connection sites primarily designed in the assembly ability are crucial for accurately achieving the desired DNA structures [19, 102].

Due to the consistency of the materials, researchers extensively studied the DNA-mediated assembly behavior using the DNA building blocks in the initial stage. These special basic units simultaneously containing the main structures and connection ligands can effectively avoid numerous preliminary preparation procedures, and facilitate the subsequent thermodynamic assembly. Mao's group has conducted comprehensive and systematic researches on the construction of 2D planar structures. Based on different kinds of N-point-star motifs with SEs extended from the branched arms, they precisely realized various large-scale 2D arrays with periodic arrangements. With three-, four-, and six-point-star DNA monomers, Mao et al. successfully obtained hexagonal, square, and 6-fold rotational symmetry 2D planes, respectively [76–78]. The sizes of each 2D arrays can readily exceed 50 μm. It is worth mentioning that the sizes of the hexagonal 2D structures assembled by the motifs with the least number of DNA arms can reach 1 mm, while maintaining a high degree of order. Furthermore, Mao's group redesigned the N-point-star motifs by introducing the interbranch "bridges" between each adjacent branched DNA arms. This innovative design can impart certain flexibility to the DNA tiles, while maintaining the rigid sufficient to construct assemblies. In 2019, the redesigned five- and six-point-star DNA motifs were utilized to form 2D quasicrystals that are highly ordered materials without translation periodicity (Fig. 8(a)) [103]. For five-point-star DNA motifs, which are required allow for a wide adjustment of angles between adjacent branches, the corresponding bridges are designed as 20-base-pair double helices with three free nucleotides at each end. These meticulous designs allow the angles between branched arms to be intelligently controlled between 60° and 90°, exactly meeting the requirements in crystallization of quasicrystals. While for six-point-star motifs, the number of the free nucleotides is reduced to one guaranteeing the angles always at ~ 60°. In the crystallization process, the five- and six-point-star monomers were mixed at specific ratios to achieve quasicrystals. At the ratio of 90:10 and 80:20, dodecagonal quasicrystals can be formed, while the ratio reaches 70:30, the mixtures containing both quasicrystals and crystals were produced. The rational strategy here provides a new access to smartly balance the rigidity and flexibility of DNA monomers, dramatically expanding the assembly ability of DNA materials. Compared to the regular junctions mentioned above, few researches are focused on the mesojunction motifs at present. In this context, Wei's group systematically explored the multi-dimensional assembly based on a series of mesojunction motifs, and successfully constructed diverse periodic lattices and composite architectures [104].

Moreover, DNA monomers can also be programmably guided to form 3D assemblies, including confined and non-confined structures. Actually, the confined 3D structures may be more visually similar to a cluster with larger sizes. As aforementioned, the three-point-star motifs have been experimentally demonstrated to enable the realization of 2D arrays with well-defined order. Despite this, the three-point-star monomers also possess the potential to construct closed polyhedral structures, when researchers simultaneously changed its design and reaction environments [105]. In the report, researchers deliberately added up the curvatures existing in the assembly, lower the monomer concentrations, and increase the flexibility of motifs, and programmably realized the tetrahedron, dodecahedron, and buckyball by precisely. Furthermore, Mao and his co-workers proposed a brand new strategy to realize the construction of more structurally complex DNA nanostructures by breaking the symmetries of the assembly monomers [106]. Additionally, they summarized a series of rules to promote the assembly of predicted structures, such as the longer loop can allow the smaller angles between flanking branched arms. In this work, three-arm branched junctions were still adapted as the building blocks. Demonstrated by the atomic force microscopy (AFM) and cryoEM, three different kinds of closed polyhedral structures, including truncated octahedron, truncated cube, and truncated cuboctahedron (Fig. 8(b), from the top bottom), were successfully obtained. Similarly, numerous researches have also been devoted to explore constructing 3D DNA architectures without boundary constraints, which is the initially intended goal of the DNA nanotechnology. After many attempts, Seeman's group ultimately realized 3D DNA crystals with 4 Å resolution using DNA tensegrity triangle tiles (Fig. 8(c)) [107]. Different from the DNA tiles utilized in previous reports, the six SEs installed at the DNA tensegrity triangle tiles cannot share the same plane, which enables the assemblies to be expanded in a 3D manner. Mao's group has once used the units with the similar shape to build materials. However, only two SEs or four SEs can be designed to project from each monomer, resulting in the final assembly being constrained in 1D and 2D [30]. The strategy for fabricating 3D DNA crystals provided by Seeman's group exhibits high scalability. Researchers can readily achieve distinct crystals by adjusting the sequences used to form DNA tensegrity triangle tiles. However, the

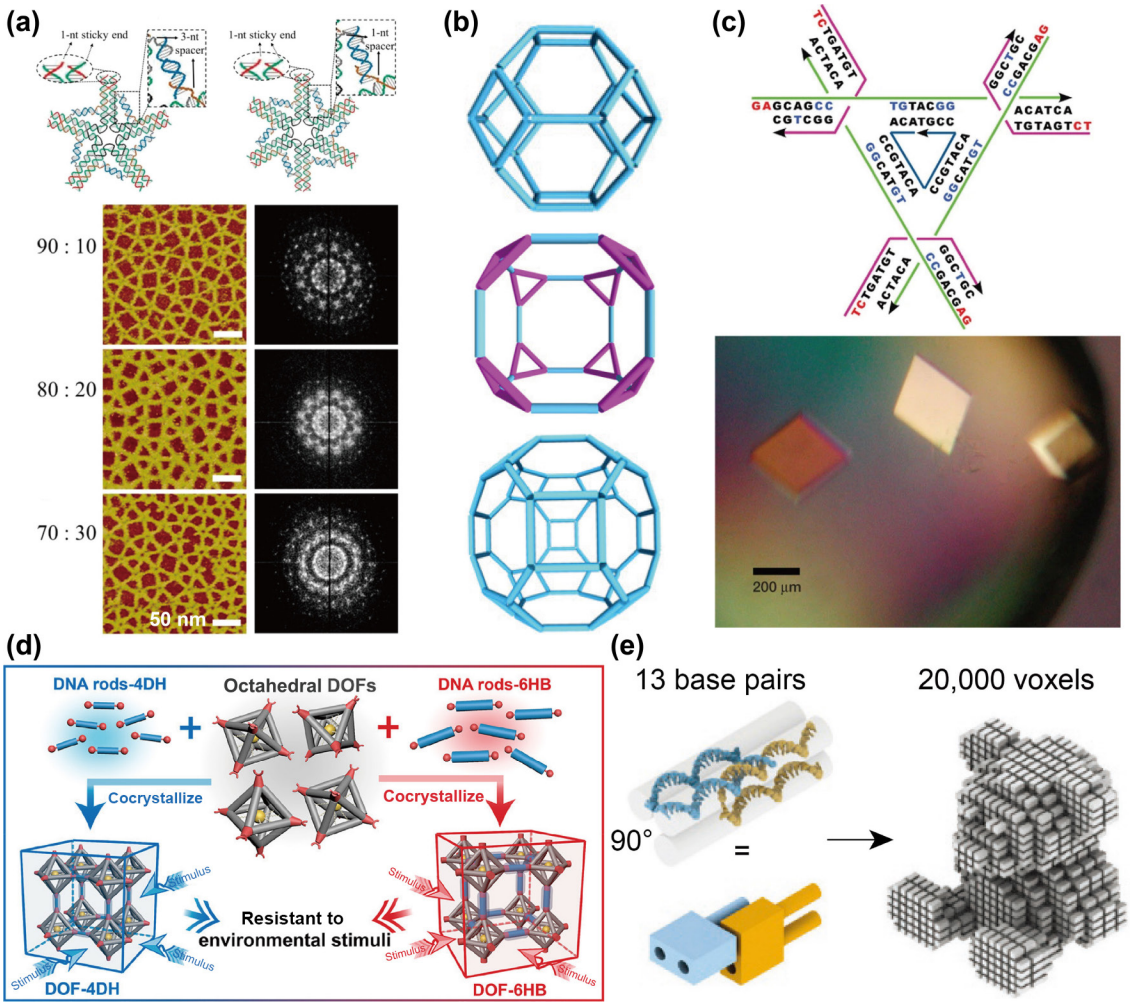

Figure 8 Simple DNA strand-mediated DNA assemblies. (a) Using five- and six-point-star motifs with flexible angles to construct 2D quasicrystals. Reproduced with permission from Ref. [103], © American Chemical Society 2019. (b) DNA polyhedral structures: truncated octahedron, truncated cube, and truncated cuboctahedron (from the top bottom). Reproduced with permission from Ref. [106], © American Chemical Society 2016. (c) Single DNA crystals (bottom) composed of DNA tensegrity triangles (top). Reproduced with permission from Ref. [107], © Macmillan Publishers Limited 2009. (d) Crystallizing AuNP/DNA origami using DNA rods. Reproduced with permission from Ref. [109], © American Chemical Society 2021. (e) The teddy bear assembled by numerous single 52-nucleotide DNA strands. Reproduced with permission from Ref. [111], © Macmillan Publishers Limited 2017.

internal cavity of this crystal is relatively narrow, which results in the failure in accommodating nanoparticles such as proteins. In this context, Yan's group proposed many excellent strategies in a targeted way, and realized the construction of 3D crystals with different structures, further promoting the problem-solving process [108].

In the assembly systems discussed above, the assembly components involved are relatively simple, and hence the single-stranded DNA is commonly considered as the inducing ligands. While for the assembly systems composed of multiple different units, the relatively complex simple DNA structures are preferred to serve as the inducing ligands. In 2021, Tian et al. proposed that rigid DNA tiles can be introduced into the 3D assembly replacing the single-stranded DNA as SEs, which can effectively adjust the superlattice constants and increase structural rigidity of 3D architectures (Fig. 8(d)) [109]. The Tian's group successfully realized the crystallization of composites composed of DNA origami and AuNPs by using different DNA nanorods varying in the thicknesses and lengths. The environmental tolerance of the crystals has been significantly improved, which can be transferred to various extreme environments, such as the solution composed of ~ 20% ethanol and ~ 12.5 mM magnesium acetate while maintaining the lattice constants almost unchanged. These progresses can promote the fabrication of designable superlattices with a wide range of application scenarios. Interestingly, in the case of the assembly of DNA structures mediated by DNA, a particularly special mechanism should be discussed here. In 2012, Yin's group described a general approach for fabricating 3D architectures using short single-stranded DNA [110]. It is worth emphasizing that the single DNA strands called "bricks" here can simultaneously serve as the main body and the connection sites, blurring the distinction between functional and non-functional areas and maximizing the utilization of DNA. Under this method, more than one hundred types of 3D architectures have been precisely fabricated as pre-designed. Furthermore, under the condition of maintaining the initial construction mode, Yin's group replaced the 32-nucleotide DNA strands by the single-stranded DNA with the length of 52 nucleotides in the assembly to achieve 3D architectures composed of larger molecular weight (Fig. 8(e)) [111]. In this work, more unique 3D assemblies with more complex structures have been almost arbitrarily constructed. The successful increase in the

component complexity indicates the endless possibilities in the structure construction and functional applications.

Simple DNA structures have also been applied to programmably guide non-DNA nanoparticles to deliberately construct architectures, especially for the 3D assemblies [112–116]. The systematic exploration of using DNA to induce 3D assembly of non-DNA nanoparticles can be traced back to last century. Throughout the years, scientists seek to assemble nanoparticles into 3D structures to further explore the collective properties emerging in such assemblies. In 1996, Mirkin et al. developed a novel strategy that has been continuously used since to rationally and reversibly assemble AuNPs into 3D aggregates [117]. They first modified two types of single-stranded DNA complementary to each other onto the AuNPs, respectively. It is worth mentioning that each DNA is functionalized with alkane thiols to enable the connection with AuNPs. These two groups of AuNPs with complementary sequences were then mixed and subjected to thermal annealing to form 3D assembly. However, the aggregates produced here cannot show periodic arrangements. It was not until 2008 that researchers utilized DNA successfully crystallizing AuNPs. Gang's group [118] and Mirkin's group [119] simultaneously reported their success in the journal of Nature. Gang and his co-workers adapted the DNA ligand design similar to the one reported in 1996 (Fig. 9(a)). The ligands are composed of two parts, the spacer and the linker. The spacer is mainly used to control the spatial distances between nanoparticles balancing the repulsion and attraction in the systems, while the linker is utilized to realize the connection between building blocks. Five different designs of DNA ligands were adapted in the experiments, among which the two types of ligands with relatively longer spacers promote the 3D assembly showing excellent periodicity. Mirkin and co-workers changed the original design of ligands by introducing additional DNA strands that can bind to the DNA modified on AuNPs and realize the interconnection task simultaneously (Fig. 9(b)). By adjusting the types of the DNA ligands, Mirkin's group programmably crystallized the AuNPs into face-centered cubic (FCC) and BCC structures based on unary and binary systems, respectively. The experimental results obtained by Gang's group and Mirkin's group both solidly reveal that the design of DNA ligands can have profound impact on the ultimate assembly results, including the degree of order and crystal structures. Conversely, this also means that the DNA-mediated assembly has huge potential for encoding

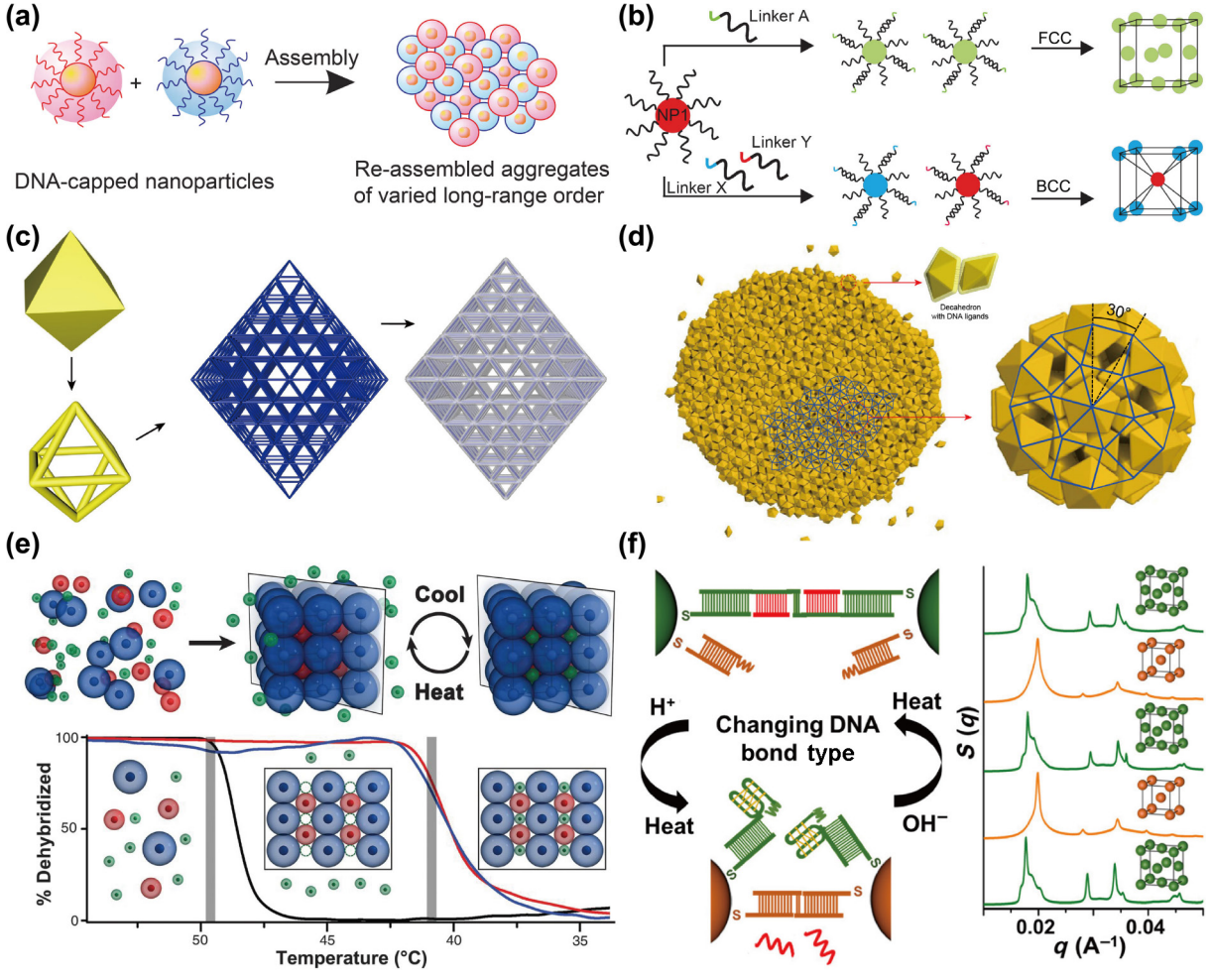

Figure 9 DNA-guided nanoparticle crystallization. (a) Crystallizing nanoparticles by single-stranded DNA. Reproduced with permission from Ref. [118], © Macmillan Publishers Limited 2008. (b) Assembling nanoparticles into crystals with FCC and BCC structures. Reproduced with permission from Ref. [119], © Macmillan Publishers Limited 2008. (c) The process to construct open-channel nanoparticle superlattices. Reproduced with permission from Ref. [122], © Macmillan Publishers Limited 2022. (d) Colloidal quasicrystals composed of decahedral nanoparticles. Reproduced with permission from Ref. [123], © Macmillan Publishers Limited 2023. (e) Dynamic ternary nanoparticle superlattices. Reproduced with permission from Ref. [125], © The American Association for the Advancement of Science 2013. (f) The pH-responsive nanoparticle 3D assembly. Reproduced with permission from Ref. [126], © American Chemical Society 2018.

nanoparticle assembly. In the subsequent decade, numerous types of 3D nanoparticles superlattices varying in the unit types, crystalline parameters, and crystallization strategies have been programmably fabricated with remarkable long-range order. In 2008, Hill et al. precisely controlled the interparticle distance in FCC crystals by adjusting the length of duplex DNA linkers [120]; in 2010, Jones et al. used different types of anisotropic nanoparticles, such as rhombic dodecahedra AuNPs, successfully constructing BCC and FCC superlattices [112]; in 2018, Lin et al. innovatively combined the DNA-meditated nanoparticle crystallization with top-down lithography, realizing the cocrystallization of spherical, cubic, and disk-shaped AuNPs [121]. This series of advances achieved in DNA-mediated assembly technology has dramatically promoted the improvement of materials manipulation with nanometer precision. With the in-depth study of crystals composed of solid monomers, the porous colloidal superlattices offering more advantages in molecular absorption gradually have attracted extensive attention from researchers. Mirkin's group provided a general strategy to construct open-channel superlattices using hollow AuNPs [122]. For the synthesis of frame nanoparticles: they first employed the selective growth of platinum to create pure platinum frames using AuNPs with specific shapes as a template, and then overgrew gold onto the platinum frames to synthesize frame nanoparticles (Fig. 9(c), left). For the fabrication of open-channel superlattices: the synthesized hollow nanoparticles were modified by DNA, and then subjected to a slow annealing to achieve the desired superlattices (Fig. 9(c), middle). With this universal strategy, twelve distinct open-channel nanoparticle superlattices have been successfully achieved. Scanning electron microscopy (SEM) were adapted to experimentally demonstrate that these achieved superlattices remain well-defined after encapsulated by silica or stabilized with Ag^+ (Fig. 9(c), right). These successful experimental cases of open-channel superlattices offer a brand new path to build functional devices, such as the negative refractive index metamaterials. Except for the 3D crystals with translational periodicity, the programmability of DNA also enables the fabrication of quasicrystals consisting of colloidal nanoparticles, which are difficult to achieve by deliberate design. Based on decahedral nanoparticles with five-fold symmetry, Mirkin and his coworkers used flexible and short DNA strands to deliberately guide the assembly of quasicrystals with 12-fold axis (Fig. 9(d)) [123]. It is worth emphasizing that, without the DNA modified on the surface, decahedral nanoparticles prefer to form the products of triclinic structures with the assembly method of drying. The single-component dodecagonal quasicrystals reported here are the first successful experimental case by deliberately assembling the colloidal nanoparticles via DNA, which establishes a solid foundation and provides an excellent model for the future realization of various types of 3D quasicrystals guided by DNA.

Except for colloidal crystals with fixed crystalline parameters, stimulus-responsive 3D nanoparticle superlattices, which can realize reversible and reconfigurable topologies for fabricating functional devices, have also been subjected to profound and systematic investigation. In 2010, Gang's group reported a simple but efficient method to realize the reversible transformation of lattice constants [124]. The single-stranded DNA with multiple encoding regions was adapted to mediate nanoparticles to form superlattices possessing BCC structures. By introducing the fuel strands to bind with the specific encoding regions or remove the DNA strands that have been connected to the encoding region, the linkers between building blocks can freely switch between single and double DNA chains, and thus the researchers can readily control interparticle distance to adjust the lattice constants. Furthermore, DNA-mediated nanoparticle superlattices can also be dynamically adjusted between different crystalline structures. Mirkin et al. ingeniously utilized the differences of binding temperatures between different DNA linkers realizing five distinct nanoparticle superlattices (Fig. 9(e)) [125]. The two-component parent nanoparticle superlattices should be first synthesized by strong DNA linkers that can maintain hybridization at the high temperature. The third component (daughter nanoparticle) modified with weak linkers can be deliberately controlled to be intercalated into or released from the parent lattices by adjusting the environment temperatures. This universal and accessible manner offers an ideal way to achieve composite materials with tunable properties. Moreover, Mirkin's group also has attempted to use i-motif DNA strands serving as linkers to fabricate pH-responsive nanoparticle superlattices [126]. Particularly, two types of DNA strands, the i-motif strands and the common strands, were simultaneously modified on the surface of nanoparticles. When at the pH 5, the BCC lattices can be formed mediated by common DNA strands, while at the pH 8, the i-motifs can expand longer than the common strands, thus dominating the assembly to form FCC superlattices. This dynamic assembly strategy avoids the introduction of a third assembly monomer and offers a simpler manner to engineer nanoparticle superlattices with unique physical and chemical properties.

3.3.2 *Guided by DNA origami*

The creation of DNA origami fundamentally overcomes the difficulties in increasing the size of the DNA monomers synthesized by one-step synthesis method. The excellent programmability of DNA origami in terms of structural dimensions, geometric shapes, and manipulation of nanomaterials enables them to effectively serve as templates to realize various nanoparticle assemblies [127–134].

Commonly, the size of 2D DNA origami monomers can readily exceed 100 nm, providing suitable platforms for assembling nanoparticles with large sizes [135–137]. In 2011, Yan and his co-workers programmably realized the synthesis of various types of AuNR dimers using an equilateral triangle origami with the arm length of ~ 116 nm [138]. Due to the high density of DNA double helices on DNA origami surfaces, the number and position of the functionalized sites can be flexibly designed to realize the high-precision capture of AuNRs. Four different inter-angles of the AuNR dimers have been realized, including 0°, 60°, 90°, and 180°. Furthermore, researchers also seek for the possibilities of creating nanoparticle clusters of more sophisticated structures based on the platforms with larger sizes. Ding and his colleagues described a general method to generate super-DNA origami through assembling multiple DNA origami monomers. In the reports, various types of nanoparticle clusters were generated by independently or simultaneously programing spherical AuNPs and AuNRs based on the super-DNA origami, which was organized by six equilateral triangle origami (Fig. 10(a)) [139]. Additionally, DNA origami can also serve as the functional platforms to fabricate dynamic functional devices composed of plasmonic nanoparticles [140]. Liu and her co-workers subtly positioned two AuNRs perpendicular to each other onto opposite sides of the rectangle-shaped DNA structures. Five binding sites in the one side of the DNA origami were set to realize the directional walk of AuNR, which was

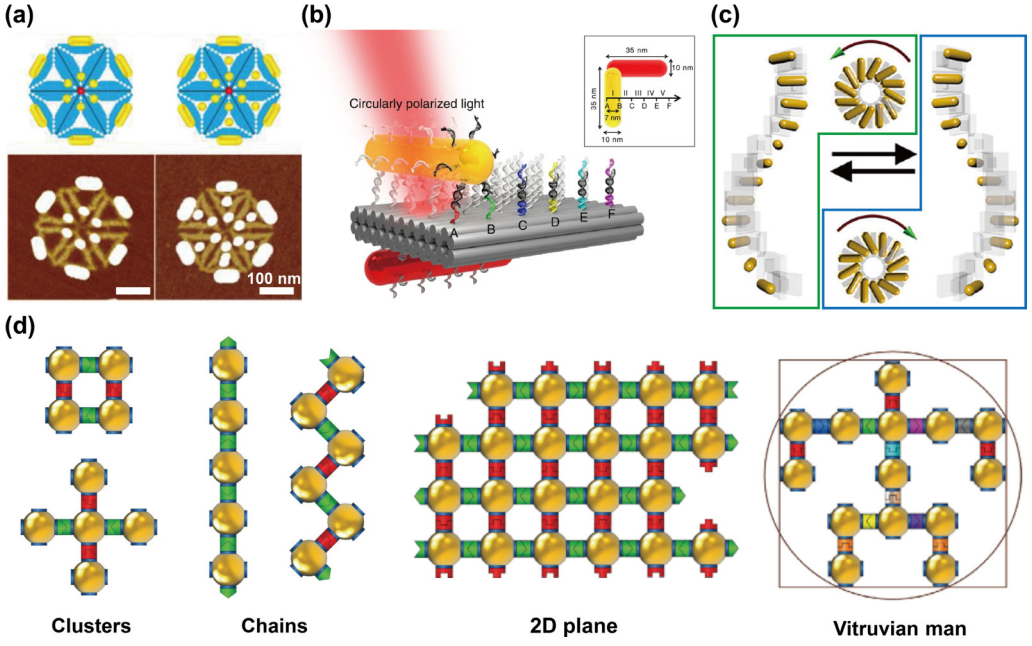

Figure 10 Various clusters and 1D, 2D assemblies based on DNA origami. (a) Clusters formed by programmably combining AuNPs and AuNRs. Reproduced with permission from Ref. [139], © American Chemical Society 2021. (b) The plasmonic walker composed of two AuNRs. Reproduced with permission from Ref. [141], © Liu, N. et al. 2015. (c) Reversible 1D helical array of AuNRs. Reproduced with permission from Ref. [142], © American Chemical Society 2018. (d) Diverse nanostructures assembled from the cross-shaped nano-objects. Reproduced with permission from Ref. [143], © Macmillan Publishers Limited 2016.

triggered by DNA strands (Fig. 10(b)) [141]. By precisely controlling the relative spatial positions of the two AuNRs, circular dichroism (CD) signals of different strengths can be obtained in real time. On the basis of the similar design idea, Lan et al. innovatively realized dynamic 1D helical structures using a well-designed V-shaped DNA origami [142]. The angle of the adjacent AuNRs can be flexibly switched between ~ 30° and ~ 120°. More ingeniously, researchers can also control the opening direction of the V-shaped origami, and the structures before and after the transformation can the exhibit mirror symmetry, which enables dramatic changes in nanodevices. In the report, the 1D helical structures were precisely constructed by connecting V-shaped DNA origami functionalized with AuNRs in a staggered manner. By adjusting the opening angle of the origami, the metallic helices can exhibit CD signals of different strength, while changing the opening direction, the researchers can readily switch chirality signals between left- and right-hand (Fig. 10(c)). This ability to achieve both refined and fundamental dynamic transformations opens up more possibilities for future applications of dynamic nanodevices. From the above description, we can keenly find that the multi-functional DNA origami monomers are the key to achieve diversified assembly. Gang et al. deliberately synthesized a rigid cross-shaped 2D monomer possessing a central hole, which is used to position the AuNP [143]. Since specific SEs can be selectively extended from each side of this origami, researchers can programmably control the assembly behavior of the composites combining origami with AuNPs to form diverse architectures, including clusters, chains, and non-confined 2D plane structures (Fig. 10(d), left). Moreover, by precisely controlling the types of assembly units and linkers projected from each building block, artificially complex structures with specific topologies, such as the Vitruvian Man, can be readily created with high-fidelity. This highly free fabrication method based on DNA origami paves a way for generating more various architectures with artificial shapes in a predictable fashion.

Additionally, DNA origami also possesses excellent 3D crystallization ability allowing for programmably directing the assembly of nanoparticles in three dimensions [144–146]. In 2016, Gang and his co-workers systematically designed various polyhedral frame structures by maximizing the designability of DNA origami [147, 148]. The shapes of these DNA origami frames (DOFs) contain tetrahedron, cube, octahedron, and so on. In the process of crystallizing nanoparticles, DOFs were deliberately controlled to serve as linkers between nanoparticles by extending SEs from each vertex. This crystallization strategy is universal for each type of the polyhedral DOFs designed here, and researchers can readily achieve different 3D nanoparticle superlattices by just simply altering the shapes of DOFs. Typically, we take the octahedral DOFs as the example to discuss the process of assembly in detail. Two types of octahedral DOFs were used in the report, regular and elongated octahedron. Under the guidance of regular octahedral DOFs, nanoparticles were directed to form FCC structures, in which the nanoparticles can connect with four vertices simultaneously in the horizontal plane, but the nanoparticles along the vertical direction can only bind to two vertices. We speculate that these structures were formed due to the planar assembly tend to form preferentially because of the relatively higher forming temperature (compared with the 1D assembly along the *z*-axis) induced by more DNA strands participating in hybridization. Similarly, the elongated octahedral DOF, of which the lengths of the edges outside the square plane are elongated, can guide the nanoparticles to form simple tetragonal (ST) superlattices. Researchers just need to simply change the draw ratio of the building blocks to obtain distinct crystals, strongly demonstrating the excellent crystallization programmability of DNA origami.

Notably, the nanoparticles are essential connection components in the 3D superlattices constructed above, which inherently limits the particle type that can participate in the 3D assembly. Hence, it is crucial to develop a strategy to realize the construction of DNA

crystal platforms as proposed by Seeman in 1982. Moreover, using the DNA origami monomers with large internal cavity to replace the simple DNA tiles as building blocks can effectively solve the problem of narrow space inside the DNA crystals. In 2020, Tian et al. provided a universal nanoparticle crystallization strategy based on the 3D platforms purely built from DOFs, fundamentally avoiding the nanoparticles to serve as the skeleton of superlattices [149]. The polyhedral DOFs are designed to project SEs from each vertex to perform 3D assembly. Different from the initial method, the SEs are used to realize the connection between polyhedral DOFs, and promote the construction of 3D platforms formed via vertex-to-vertex hybridization between DOF monomers. The functional DNA chains are projected from the inside of monomers to precisely anchor the nanoparticles into the body center of the DOFs. In the assembly process, nanoparticles are completely wrapped in the DNA origami thoroughly cutting off the connection with the outside. As shown in Fig. 10(a), Tian et al. used cubic, regular octahedral, and regular tetrahedral DOFs successfully guiding the nanoparticles to construct simple cubic (SC), BCC, and cubic diamond structures, respectively. The particles adapted in the SC superlattices were QDs, while in the other superlattices were AuNPs, strongly demonstrating the universality of this strategy across guest nanoparticle types. However, the researchers quickly discover the drawbacks that only using a single shape of DOFs for crystallization can severely limit the variety of achievable 3D platforms. Hence, Tian's group began to focus on the exploration of the cocrystallization of DOFs. At the beginning, they used two types of DOFs, the regular and elongated octahedron, to serve as building blocks [150]. Theoretically, these two DOFs can be used to realize innumerable crystal structures. However, due to the decrease in structural symmetry consistency of building blocks, the SEs are required to realize the linking between specific vertexes rather than just completing the task of connection. As an example, if the two types of DOFs are assembled in the form of alternating in 3D space, we can find that the vertices along the vertical direction of the two DOFs should bind to each other, while the other vertices should connect to each other (Fig. 11(b), left). Therefore, two types of DNA SE pairs (described in different colors) were designed to guarantee the correct assembly of superlattices (Fig. 11(b), right). Furthermore, Tian's group attempted to introduce a third DOF, the partially elongated octahedral DOF, with a different shape to realize more various nanoparticle superlattices [151]. The partially elongated octahedral DOF can be obtained by elongating the four edges that converge at one vertex of the regular octahedral DOF. With the introduction of three DOFs, the programmability of the superlattices can be dramatically improved by increasing the assembly units (not the shape type) and adjusting the spatial arrangement of the assembly units. Correspondingly, the requirements for the control accuracy of spatial relative positions between building blocks are significantly increased. Due to the further reduction of the structure symmetry of the assembly units, the SEs at the vertex in the horizontal plane were designed as four types to avoid the flipping between monomers (Fig. 11(c)). In the report, Tian's group successfully realized 38 kinds of nanoparticle superlattices using three distinct DNA platforms. Except for focusing on rationally constructing 3D assembly, Tian's group is also interested in the geometry-mediated assembly based on DNA origami [152]. In experiments, they found a surprising phenomenon that elongated octahedral DOFs can guide nanoparticles to form SC structures under the design of non-specific SEs (Fig. 11(d), left), which is intuitively considered as difficult. After a large amount of characterization and careful consideration, the flexible DNA SEs are thought to play a crucial role, which can effectively relieve the stress induced by the improper assembly. To further verify the explanations, single-stranded DNA were added to effectively improve the SE rigidity by increasing the ratio of double strands in SEs. Consistent with the envision, the nanoparticle superlattices were transformed from SC to ST structures (Fig. 11(d), right). This 3D form type satisfies the orderly arrangement of elongated octahedral DOFs and effectively avoids the accumulation of stress. The excellent 3D programmability ability exhibited by the DNA origami monomers provides more possibilities for the arbitrary crystallization of nanoparticles.

4 Applications of nanomaterial assemblies

With the exploration of nanomaterial assembly continuing to deepen, more and more well-defined nanomaterial assemblies have been programmably achieved. The emerging unique properties of the nanomaterial assemblies offer new opportunities for wide applications in various fields, including optics, catalysis, and medicine.

4.1 Optics

Colloidal noble metal nanoparticles, especially for AuNPs and AgNPs, commonly possess extensive SPR. Therefore, unique optical properties can be deliberately produced by precisely controlling the coupling between nanoparticles. The bottom-up strategies opportunely provide an ideal way to realize the controllable coupling by programmably manipulating the arrangements of nanoparticles [153–155].

DNA-mediated self-assembly provides a powerful method to controllably generate desired assembly composed of metal nanoparticles. Liedl et al. subtly constructed the helix of AuNPs with diameter of 10 nm using 24-helix bundles folded by DNA origami technology (Fig. 12(a)) [156]. By programmably adjusting the position of AuNPs around the DNA origami bundle, left- and right-handed nanoparticle helices can be readily fabricated with precise helical diameter (34 nm) and period (57 nm). Under this design, these two types of nanoparticle helices both exhibited expected but weak chiral signals, which was attributed to small nanoparticle size and large adjacent nanoparticle distance. In order to effectively enhance the chiral signals, Liedl's group utilized the manner of electroless deposition to increase the size of AuNPs already positioned on the nano bundles. After a suitable period of growth, the particle sizes were uniformly increased to 16 ± 2 nm, and the accessible chiral signals were successfully amplified 400 times highly consistent with the theoretical predictions. Furthermore, Liedl's group also attempted to use excessive silver materials with stronger SPR to grow AuNPs heterogeneously, and successfully achieved the huge molar CD with the strength up to 10^8 $M^{-1}\cdot cm^{-1}$. Additionally, the peaks of the CD signals experimentally obtained fall between 500 and 600 nm, indicating the success in fabricating optical devices with controlled response across the range of visible spectrum. Recently, Liu and her co-workers focused on the exploration of dynamic chiral devices based on the similar helical structures [157]. The AuNPs around the helix can be readily transported to the specified location using accessible strand displacement reaction. Under this strategy, the strength and

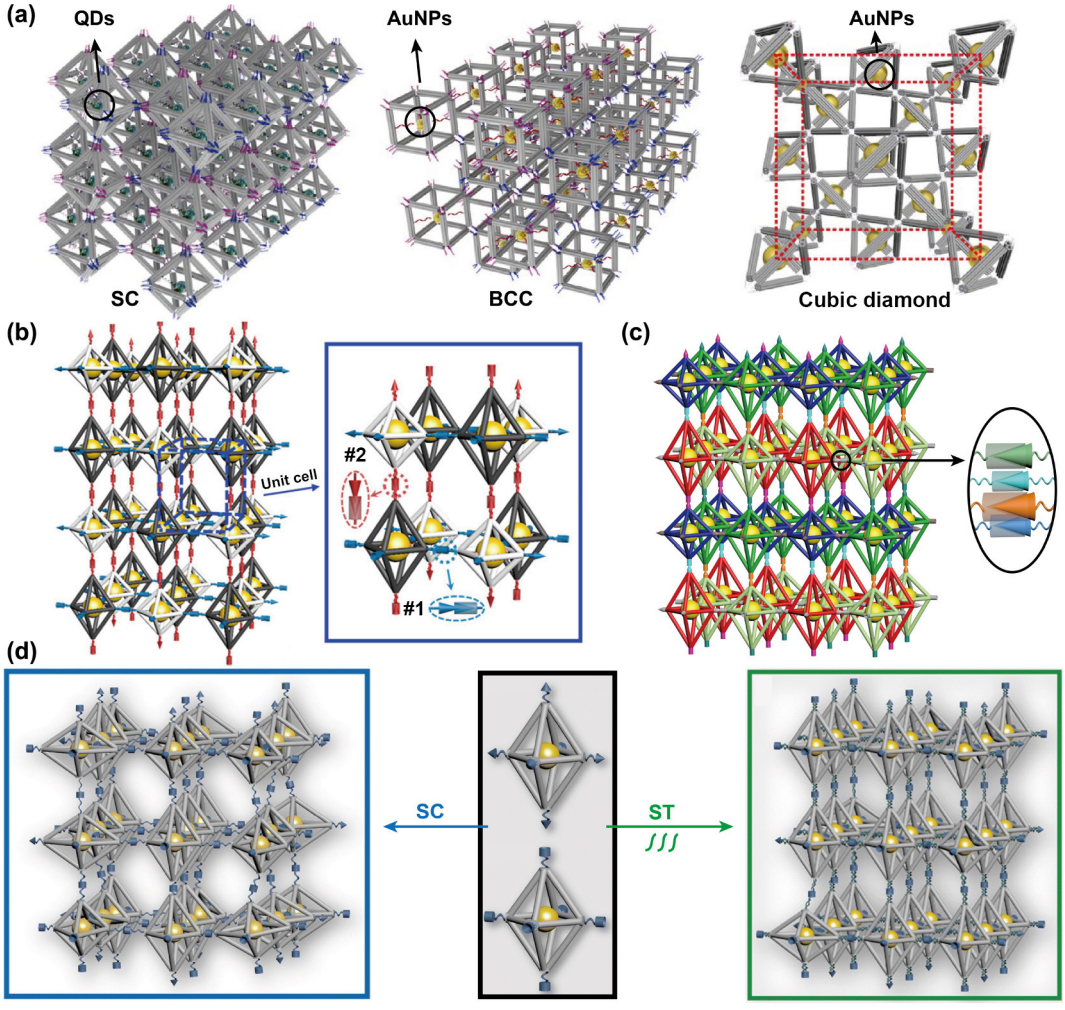

Figure 11 Programmable crystallization of nanoparticles based on DNA origami. (a) The SC, BCC, and cubic diamond nanoparticle superlattices with guest nanoparticles of QDs, AuNPs, and AuNPs, respectively (from the left right). Reproduced with permission from Ref. [149], © Macmillan Publishers Limited 2020. (b) Nanoparticle superlattices based on binary DNA origami. Reproduced with permission from Ref. [150], © American Chemical Society 2020. (c) Nanoparticle superlattices based on ternary DNA origami. Reproduced with permission from Ref. [151], © Tian, Y. et al. 2022. (d) Shape-guided crystallization of nanoparticles. Reproduced with permission from Ref. [152], © The Royal Society of Chemistry 2023.

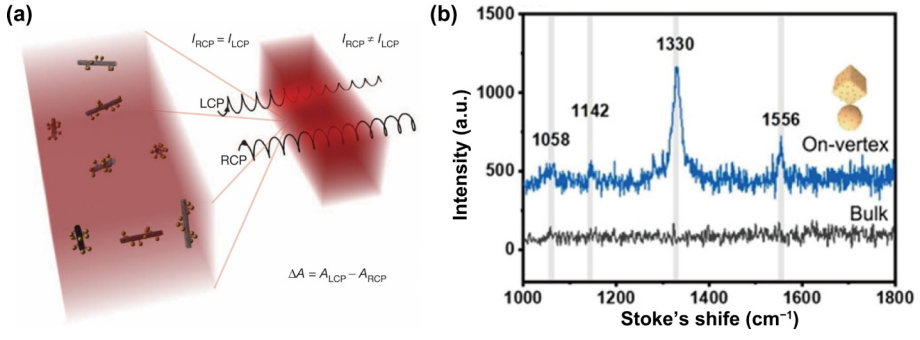

Figure 12 Different optical properties existing in the assemblies of metal nanoparticles. (a) Assembling AuNPs to form helical structures with left- and right-handed CD. Reproduced with permission from Ref. [156], © Macmillan Publishers Limited 2012. (b) The enhanced Raman scattering induced through combing spherical AuNPs with cubic AuNPs at the vertex. Reproduced with permission from Ref. [158], © Wiley-VCH GmbH, 2021.

the peak position of the CD signals can be sensitively transferred after precise manipulation.

Compared with spherical nanoparticles, cubic nanoparticles with anisotropic geometric shapes can remarkably exhibit tunable localized SPR. Dramatically enhanced Raman scattering signals can be achieved by positioning molecules in the hot-spot regions constructed by metallic nanoparticles. Wang et al. proposed an efficient strategy based on DNA origami to achieve the generation of metal clusters with different configurations [158]. When dye molecules were anchored in the connection region of the dimer generated by binding spherical nanoparticles to the cubic nanoparticles at the vertex, remarkable enhanced surface Raman scattering signals can be clearly detected (Fig. 12(b)).

4.2 Catalysis

Compared with bulk materials, colloidal nanoparticles have a higher surface-volume ratio further improving the material utilization. The intense collective effects induced by high-dimensional assemblies provide an attractive access to fabricating catalytic materials composed of nanoscale monomers [159–162].

Due to the abundant active sites, AuNPs are acknowledged as the excellent catalysts. However, the ligands playing the crucial role in assembly usually occupy a large amount of sites of nanoparticle surface, which intensely weakens corresponding catalytic activity. Hence, Mirkin's group described a simple method to re-expose the functional active sites using calcination [163]. The single-stranded DNA-mediated AuNP superlattices were first stabilized by utilizing silica encapsulation, and then the superlattices were subjected to a fast calcination for 2 h at 350 °C (Fig. 13(a)). All DNA strands were successfully calcined, which was strongly demonstrated by Fourier transform infrared spectroscopy measurements. Additionally, the 3D arrangements of nanoparticles still maintained original BCC structures. To verify the catalytic activity of the superlattices, the achieved products were added to the solution consisting of 4-hydroxybenzyl alcohol, K_2CO_3, and D_2O. After 24 h, the researchers successfully detected 79% aldehyde yield. Except for metal nanoparticles, the metal–organic framework (MOF) nanoparticles are also able to serve as the efficient catalysts in chemical reactions. To explore the practical significance of the superlattices assembled by MOF nanoparticles in catalytic reactions, Mirkin's group compared the PCN-222 2D superlattices with the corresponding microscale single crystals for photocatalysis, in which the oxidation of 2-chloroethyl ethyl sulfide (CEES) to nontoxic 2-chloroethyl ethyl sulfoxide (CEESO) was adapted as the experimental reactions [164]. To avoid the structural collapse caused by the dehybridization of double-stranded DNA linkers, Ag^+ ion was promptly added as the stabilizer to maintain the in situ porous structures of PCN-222 2D superlattices. In a reaction time of nearly 400 min, the conversion rate from CEES to CEESO catalyzed by PCN-222 2D superlattices can be clearly observed to be stably and significantly higher than that catalyzed by PCN-222 single crystals (Fig. 13(b)). This more efficient catalytic efficiency was attributed to the relative larger light absorption areas of the structures, which can be easily achieved by 2D porous crystals. Additionally, the ordered arrays of biomolecules have also been demonstrated to possess better catalytic efficiency. Gang's group selected a typical enzymatic cascade reaction, the glucose oxidase (GOx)-horseradish peroxide (HRP) pair, as the reaction model [149]. In experiments, the reaction rates of three different organizational forms (the monodisperse, disordered aggregates, and SC superlattices) of these two biomolecules with equal molar ratio were carefully detected, and the researchers could clearly observe that the form of crystal structures catalyzed the enzyme cascade reactions to the greatest extent.

4.3 Medicine

Nanomaterial self-assembly is an effective approach for constructing advanced materials within the realms of diagnosis and treatment [165]. Commonly, the complexity of the biological environment is a key factor that weakens the function of drug therapy. Therefore, diverse types of nanomaterials, including proteins, liposomes, and DNA, are introduced in exploration to cope with the changing internal environments.

Due to its excellent biodegradability, biocompatibility, biological specificity, and outstanding self-assembly ability, peptide self-assembly has been widely used in medical applications, primarily lying in medical imaging and disease treatment [166–168]. By integrating different imaging components (such as radioactive isotopes, fluorophores, etc.), imaging probes based on self-assembling peptides with high specificity have been applied to various imaging modalities. In 2024, Cai et al. described a novel approach for realizing the assembly of CD47 and CD24 dual-target inhibitors (PAC-SABI) (Fig. 14(a)) [169]. This approach can simulate the phagocytic activity of macrophages against malignant cells, efficiently inducing effective anti-tumor immunity. In addition, self-assembling peptide-based materials can also be combined with biomineralization, nanotechnology, and tissue engineering to promote the regeneration of both hard and soft tissues.

Liposomes are spherical vesicles composed of synthetic or natural phospholipids [167]. These vesicles are surrounded by a hydrophobic membrane enclosing a water core, capable of carrying various hydrophobic or hydrophilic molecules for therapeutic

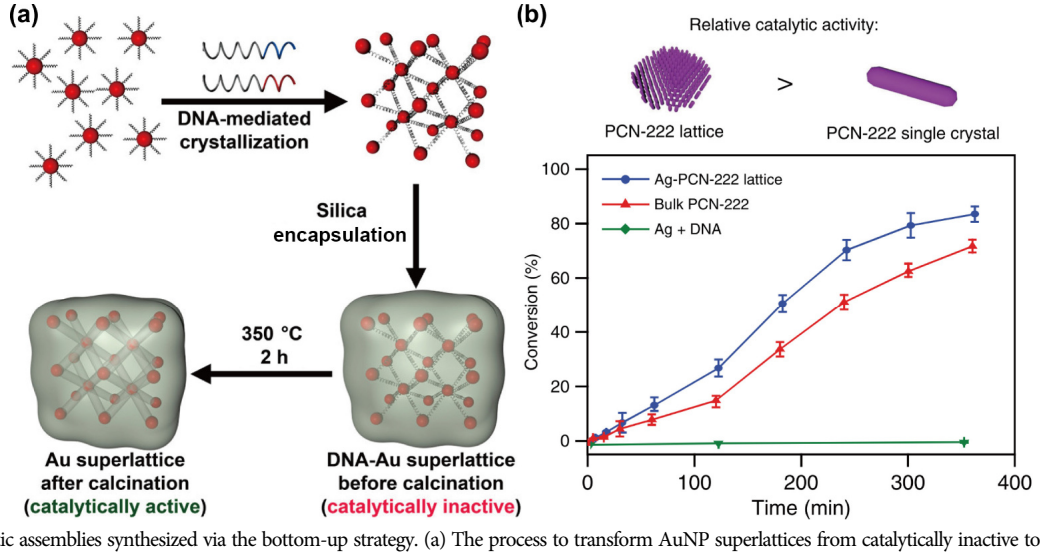

Figure 13 Catalytic assemblies synthesized via the bottom-up strategy. (a) The process to transform AuNP superlattices from catalytically inactive to catalytically active. Reproduced with permission from Ref. [163], © American Chemical Society 2015. (b) PCN-222 lattices possess better catalytic performance than PCN-222 single crystals. Reproduced with permission from Ref. [164], © Mirkin, C. A. et al. 2020.

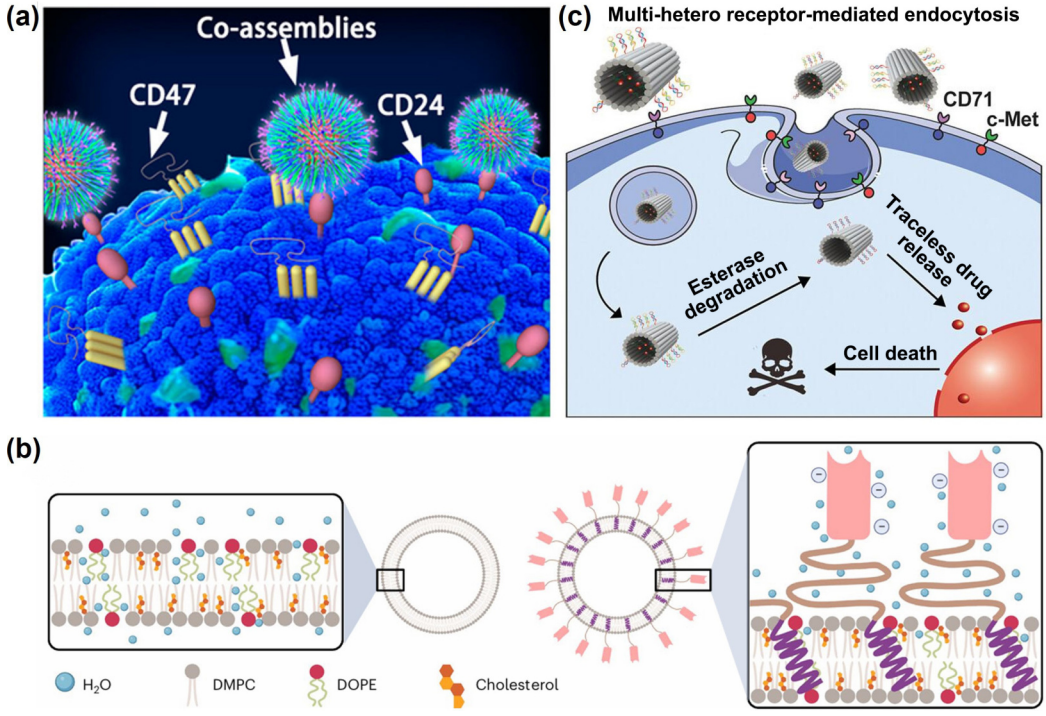

Figure 14 The application of assemblies in medicine. (a) Schematic of PAC-SABIs-mediated macrophage phagocytosis of cancer cells after assembly. Reproduced with permission from Ref. [169], © Cai, Y. B. et al. 2024. (b) Schematic of the biophysical process transition caused by the interactions between liposomes and chimeric nanobody-decorated liposomes. Reproduced with permission from Ref. [170], © Macmillan Publishers Limited 2024. (c) Schematic illustration of endocytosis mediated by multiple different receptors, with simultaneous esterase triggering for specific drug release. Reproduced with permission from Ref. [175], © American Chemical Society 2024.

purposes. Wan et al. reported a chemically modified biophysical method to produce immunoliposomes by self-assembling chimeric nanobody into the liposomal bilayer (Fig. 14(b)) [170]. In the report, researchers experimentally demonstrated that immunoliposomes loaded with drugs can inhibit the growth of xenograft tumors and improve survival rates. Additionally, they also found that the release of drugs depends on both the properties of the liposomes and the surrounding environments, including the composition of the liposomes, pH value, osmotic gradient, and related parameters of the surrounding environment.

Likewise, DNA assembly has also attracted extensive attention from researchers because of its considerable potential for application in diverse areas, including bionics, bioimaging, and drug delivery [171]. Particularly in bioimaging, DNA labeled with fluorescent markers exhibits high specificity in recognition, enabling high-precision microscopic imaging of the interior of the human body. Luo et al. successfully synthesized nanorods encoded with fluorescence intensity based on dendritic molecular-like DNA [172]. The corresponding multiplex detection of several pathogenic DNA can be achieved with high sensitivity, rapidity, and stability. DNA assemblies can also be utilized as drug carriers, facilitating the targeted delivery within cells. Compared with other drug carriers, the principal advantages of DNA assemblies as drug carriers include the designability of molecules, membrane permeability, and addressability [171, 173]. Zhao's group synthesized DNA robots to serve as the molecular trigger. The exterior of the DNA robot was functionalized with DNA aptamers, allowing for effectively programming to transport and specifically release thrombin in tumor blood vessels, inducing intravascular thrombosis leading to tumor necrosis and further inhibiting tumor growth [174]. Additionally, Zhang's group devised various adjustable DNA structures based on multivalent aptamers [175]. The precise control of the type, valency, and geometric pattern of aptamers reveals that multi-hetero-receptor-mediated recognition not only facilitates the specific recognition of DNA origami structures with tumor cells but also significantly enhances cellular uptake.

5 Summary and outlook

Over the past twenty years, promoted by the rapid development of nanomaterial synthesis technology and the ongoing innovation in assembly techniques, substantial and far-reaching progress has been made in the bottom-up assembly methodologies, particularly in DNA-mediated self-assembly. An increasing variety of nanoparticles including AuNPs, AgNPs, QDs, DNA structures, etc. can be readily prepared with different sizes and shapes, dramatically enriching the types of building blocks used for constructing nanostructures. Moreover, different ligands with flexible configurations robustly provide numerous effective bridges for constructing multi-dimensional assemblies with distinct performances through weak interactions. Particularly, DNA structures ranging from simple strands to complex origami have been extensively utilized to precisely program the nanoparticle assembly. Leveraging the precise control inherent in DNA, nanomaterials of various forms can be programmably guided to achieve a series of assemblies with nanoscale precision, including clusters, 1D chains, 2D planes, and 3D superlattices. Compared with other ligands, DNA has exhibited exceptional programmability in manipulating the spatial relative positions between nanomaterials by adjusting the particle distance, arrangement type etc., and hundreds of different nanoparticle superlattices spanning dozens 3D symmetries have been

successfully realized. Various fields achieve interdisciplinary integration through bottom-up assembly as a connecting link. The hence realized assemblies have been extensively applied in optical devices, catalysis, medicine and so on. Compared to clusters, nanoarrays with higher particle density offer significant advantages in enhancing the collective effect of nanoparticles. Nanoparticles with SPR can be effectively organized into 1D helical arrays, including those with dynamic structures. According to the directionality of the helix, different chiral signals can be realized. The directionality of the helix enables the generation of distinct chiral signals, which can be further amplified or diminished by adjusting the number of nanoparticle units. In 2D arrays, the nanoparticles can be arranged into periodic porous structures. For nanoparticles with photocatalytic properties, such as MOF, these corresponding 2D arrays can improve catalytic performance by increasing the effective light absorption area. Different from 1D and 2D arrays, 3D arrays can compactly assemble nanoparticles within a confined space, significantly boosting particle density. This higher density allows for enhanced collective effects, leading to superior functional properties such as improved catalysis and optical performance. Moreover, the 3D arrays offer more adjustable parameters, which can make them highly versatile for applications across a broader range of scenarios.

Although a series of significant advancements have been achieved in bottom-up assembly, it remains a challenge to deliberately design and fabricate low-symmetry 3D nanoparticle superlattices in an arbitrary way, as it demands strict assembly accuracy and diverse 3D spatial control. The emerging "locked mode" of the DNA SE design may provide an accessible way towards the creation of artificially complicated nanostructures. Furthermore, we believe that researches should also focus on the synthesis of high-quality materials with various properties, such as optics, magnetism, electricity, etc. The exceptional capacity of DNA structures to host guest nanoparticles offers a promising pathway for synthesizing materials with tailored properties. By simultaneously integrating diverse functional nanoparticles into multi-dimensional DNA-based structures, materials with multiple functions can be effectively developed. For example, nanoparticles, such as AuNPs and titanium dioxide nanoparticles, hold potential for assembling into materials that simultaneously exhibit optical and catalytic properties. Additionally, leveraging the programmability of DNA can enable the reversible and precise adjustment of nanoparticle parameters, such as relative positions, to activate or deactivate, as well as enhance or diminish, specific functionalities. It is worth emphasizing that the exploration of properties is driven by the goal of achieving practical applications. Hence, a mature and industrialized assembly methodology for preparing specific materials is a prerequisite, which can guarantee the high yield of assemblies. Continued efforts are also anticipated to put into exploring how to effectively expand the assembly sizes to stably achieve hundred-micron or even millimeter-scale materials under the bottom-up methodology. These large-scale materials can facilitate the subsequent manipulation from the top down and the fabrication of devices with high-throughput signals. We believe that, with the continuous development of the bottom-up assembly technology, more various materials with powerful functions will be integrated in daily life.

Data availability

Not applicable.

Acknowledgements

This work is supported by the Natural Science Foundation of Jiangsu Province (No. BK20220124), the Fundamental Research Funds for the Central Universities (No. 2024300319), the National Natural Science Foundation of China (No. 22372077 and 92356304), the Postdoctoral Fellowship Program of CPSF (No. GZB20240302), the funding from State Key Laboratory of Analytical Chemistry for Life Science (No. 5431ZZXM2301), and the Program for Outstanding PhD Candidates of Nanjing University (Nos. 202401A12 and 202401B06).

Declaration of competing interest

All the contributing authors report no conflict of interests in this work.

Author contribution statement

M. J.: Supervision, writing – original draft, writing – review & editing. H. Y. G.: Writing – original draft, writing – review & editing. M. S. P.: Writing – review & editing. P. X. L.: Writing – review & editing. X. L. X.: Writing – review & editing. Z. Y. Z.: Writing – review & editing. X. X. H.: Writing – review & editing. Y. T.: Conceptualization, funding acquisition, supervision, writing – review & editing. All the authors have approved the final manuscript.

Use of AI statement

None.

References

[1] Rosi, N. L.; Mirkin, C. A. Nanostructures in biodiagnostics. *Chem. Rev.* **2005**, *105*, 1547–1562.

[2] Zhang, Q.; Li, N.; Goebl, J.; Lu, Z. D.; Yin, Y. D. A systematic study of the synthesis of silver nanoplates: Is citrate a "magic" reagent. *J. Am. Chem. Soc.* **2011**, *133*, 18931–18939.

[3] Langille, M. R.; Zhang, J.; Personick, M. L.; Li, S. Y.; Mirkin, C. A. Stepwise evolution of spherical seeds into 20-fold twinned icosahedra. *Science* **2012**, *337*, 954–957.

[4] Ke, Y. G.; Voigt, N. V.; Gothelf, K. V.; Shih, W. M. Multilayer DNA origami packed on hexagonal and hybrid lattices. *J. Am. Chem. Soc.* **2012**, *134*, 1770–1774.

[5] Li, J. X.; Zhu, Z.; Liu, F.; Zhu, B. Q.; Ma, Y. L.; Yan, J. M.; Lin, B. Q.; Ke, G. L.; Liu, R. D.; Zhou, L. J. et al. DNA-mediated morphological control of silver nanoparticles. *Small* **2016**, *12*, 5449–5487.

[6] Winfree, E.; Liu, F. R.; Wenzler, L. A.; Seeman, N. C. Design and self-assembly of two-dimensional DNA crystals. *Nature* **1998**, *394*, 539–544.

[7] Ding, B. Q.; Deng, Z. T.; Yan, H.; Cabrini, S.; Zuckermann, R. N.; Bokor, J. Gold nanoparticle self-similar chain structure organized by DNA origami. *J. Am. Chem. Soc.* **2010**, *132*, 3248–3249.

[8] Pal, S.; Deng, Z. T.; Ding, B. Q.; Yan, H.; Liu, Y. DNA-origami-directed self-assembly of discrete silver-nanoparticle architectures. *Angew. Chem., Int. Ed.* **2010**, *49*, 2700–2704.

[9] Wei, J.; Wang, H.; Deng, Y. H.; Sun, Z. K.; Shi, L.; Tu, B.; Luqman, M.; Zhao, D. Y. Solvent evaporation induced aggregating assembly approach to three-dimensional ordered mesoporous silica with ultralarge accessible mesopores. *J. Am. Chem. Soc.* **2011**, *133*, 20369–20377.

[10] Truong-Quoc, C.; Lee, J. Y.; Kim, K. S.; Kim, D. N. Prediction of

DNA origami shape using graph neural network. *Nat. Mater.* **2024**, *23*, 984–992.

[11] Jin, H.; Livache, C.; Kim, W. D.; Diroll, B. T.; Schaller, R. D.; Klimov, V. I. Spin-exchange carrier multiplication in manganese-doped colloidal quantum dots. *Nat. Mater.* **2023**, *22*, 1013–1021.

[12] Wang, Y.; Chen, J.; Zhong, Y. X.; Jeong, S.; Li, R. P.; Ye, X. C. Structural diversity in dimension-controlled assemblies of tetrahedral gold nanocrystals. *J. Am. Chem. Soc.* **2022**, *144*, 13538–13546.

[13] Diroll, B. T.; Fedin, I.; Darancet, P.; Talapin, D. V.; Schaller, R. D. Surface-area-dependent electron transfer between isoenergetic 2D quantum wells and a molecular acceptor. *J. Am. Chem. Soc.* **2016**, *138*, 11109–11112.

[14] Xue, C.; Hu, S. Y.; Gao, Z. H.; Wang, L.; Luo, M. X.; Yu, X.; Li, B. F.; Shen, Z. F.; Wu, Z. S. Programmably tiling rigidified DNA brick on gold nanoparticle as multi-functional shell for cancer-targeted delivery of siRNAs. *Nat. Commun.* **2021**, *12*, 2928.

[15] Wang, Y. J.; Peng, L. C.; Schreier, J.; Bi, Y.; Black, A.; Malla, A.; Goossens, S.; Konstantatos, G. Silver telluride colloidal quantum dot infrared photodetectors and image sensors. *Nat. Photon.* **2024**, *18*, 236–242.

[16] O'Brien, M. N.; Jones, M. R.; Lee, B.; Mirkin, C. A. Anisotropic nanoparticle complementarity in DNA-mediated co-crystallization. *Nat. Mater.* **2015**, *14*, 833–839.

[17] Tian, Y.; Wang, T.; Liu, W. Y.; Xin, H. L.; Li, H. L.; Ke, Y. G.; Shih, W. M.; Gang, O. Prescribed nanoparticle cluster architectures and low-dimensional arrays built using octahedral DNA origami frames. *Nat. Nanotechnol.* **2015**, *10*, 637–644.

[18] Jiang, S. X.; Pal, N.; Hong, F.; Fahmi, N. E.; Hu, H. Y.; Vrbanac, M.; Yan, H.; Walter, N. G.; Liu, Y. Regulating DNA self-assembly dynamics with controlled nucleation. *ACS Nano* **2021**, *15*, 5384–5396.

[19] Tikhomirov, G.; Petersen, P.; Qian, L. L. Fractal assembly of micrometre-scale DNA origami arrays with arbitrary patterns. *Nature* **2017**, *552*, 67–71.

[20] Macfarlane, R. J.; Lee, B.; Jones, M. R.; Harris, N.; Schatz, G. C.; Mirkin, C. A. Nanoparticle superlattice engineering with DNA. *Science* **2011**, *334*, 204–208.

[21] O'Brien, M. N.; Girard, M.; Lin, H. X.; Millan, J. A.; Olvera de la Cruz, M.; Lee, B.; Mirkin, C. A. Exploring the zone of anisotropy and broken symmetries in DNA-mediated nanoparticle crystallization. *Proc. Natl. Acad. Sci. USA* **2016**, *113*, 10485–10490.

[22] Nguyen, L.; Dass, M.; Ober, M. F.; Besteiro, L. V.; Wang, Z. M.; Nickel, B.; Govorov, A. O.; Liedl, T.; Heuer-Jungemann, A. Chiral assembly of gold-silver core-shell plasmonic nanorods on DNA origami with strong optical activity. *ACS Nano* **2020**, *14*, 7454–7461.

[23] Vietz, C.; Kaminska, I.; Sanz Paz, M.; Tinnefeld, P.; Acuna, G. P. Broadband fluorescence enhancement with self-assembled silver nanoparticle optical antennas. *ACS Nano* **2017**, *11*, 4969–4975.

[24] Holzmeister, P.; Pibiri, E.; Schmied, J. J.; Sen, T.; Acuna, G. P.; Tinnefeld, P. Quantum yield and excitation rate of single molecules close to metallic nanostructures. *Nat. Commun.* **2014**, *5*, 5356.

[25] Sánchez-Iglesias, A.; Winckelmans, N.; Altantzis, T.; Bals, S.; Grzelczak, M.; Liz-Marzán, L. M. High-yield seeded growth of monodisperse pentatwinned gold nanoparticles through thermally induced seed twinning. *J. Am. Chem. Soc.* **2017**, *139*, 107–110.

[26] Cheng, Z. H.; Jones, M. R. Assembly of planar chiral superlattices from achiral building blocks. *Nat. Commun.* **2022**, *13*, 4207.

[27] Stamplecoskie, K. G.; Scaiano, J. C. Light emitting diode irradiation can control the morphology and optical properties of silver nanoparticles. *J. Am. Chem. Soc.* **2010**, *132*, 1825–1827.

[28] Lan, X. Z.; Chen, M. L.; Hudson, M. H.; Kamysbayev, V.; Wang, Y. Y.; Guyot-Sionnest, P.; Talapin, D. V. Quantum dot solids showing state-resolved band-like transport. *Nat. Mater.* **2020**, *19*, 323–329.

[29] Ossia, Y.; Levi, A.; Panfil, Y. E.; Koley, S.; Scharf, E.; Chefetz, N.; Remennik, S.; Vakahi, A.; Banin, U. Electric-field-induced colour switching in colloidal quantum dot molecules at room temperature. *Nat. Mater.* **2023**, *22*, 1210–1217.

[30] Liu, D. G.; Wang, M. S.; Deng, Z. X.; Walulu, R.; Mao, C. D. Tensegrity: Construction of rigid DNA triangles with flexible four-arm DNA junctions. *J. Am. Chem. Soc.* **2004**, *126*, 2324–2325.

[31] Qian, H.; Tian, C.; Yu, J. W.; Guo, F.; Zheng, M. S.; Jiang, W.; Dong, Q. F.; Mao, C. D. Self-assembly of DNA nanotubes with defined diameters and lengths. *Small* **2014**, *10*, 855–858.

[32] Han, D. R.; Pal, S.; Yang, Y.; Jiang, S. X.; Nangreave, J.; Liu, Y.; Yan, H. DNA gridiron nanostructures based on four-arm junctions. *Science* **2013**, *339*, 1412–1415.

[33] Zhou, Y. H.; Dong, J. Y.; Zhou, C.; Wang, Q. B. Finite assembly of three-dimensional DNA hierarchical nanoarchitectures through orthogonal and directional bonding. *Angew. Chem., Int. Ed.* **2022**, *61*, e202116416.

[34] Kimchi, O.; Goodrich, C. P.; Courbet, A.; Curatolo, A. I.; Woodall, N. B.; Baker, D.; Brenner, M. P. Self-assembly-based posttranslational protein oscillators. *Sci. Adv.* **2020**, *6*, eabc1939.

[35] Du, M. M.; Zhou, K.; Yu, R. Z.; Zhai, Y. F.; Chen, G.; Wang, Q. B. Noncovalent self-assembly of protein crystals with tunable structures. *Nano Lett.* **2021**, *21*, 1749–1757.

[36] Liu, H.; Matthies, M.; Russo, J.; Rovigatti, L.; Narayanan, R. P.; Diep, T.; McKeen, D.; Gang, O.; Stephanopoulos, N.; Sciortino, F. et al. Inverse design of a pyrochlore lattice of DNA origami through model-driven experiments. *Science* **2024**, *384*, 776–781.

[37] DeLuca, M.; Duke, D.; Ye, T.; Poirier, M.; Ke, Y. G.; Castro, C.; Arya, G. Mechanism of DNA origami folding elucidated by mesoscopic simulations. *Nat. Commun.* **2024**, *15*, 3015.

[38] Kim, B.; Tripp, S. L.; Wei, A. Self-organization of large gold nanoparticle arrays. *J. Am. Chem. Soc.* **2001**, *123*, 7955–7956.

[39] Sun, Y.; Xia, Y. Triangular nanoplates of silver: Synthesis, characterization, and use as sacrificial templates for generating triangular nanorings of gold. *Adv. Mater.* **2003**, *15*, 695–699.

[40] Kim, A.; Vo, T.; An, H.; Banerjee, P.; Yao, L. H.; Zhou, S.; Kim, C.; Milliron, D. J.; Glotzer, S. C.; Chen, Q. Symmetry-breaking in patch formation on triangular gold nanoparticles by asymmetric polymer grafting. *Nat. Commun.* **2022**, *13*, 6774.

[41] Turkevich, J.; Stevenson, P. C.; Hillier, J. A study of the nucleation and growth processes in the synthesis of colloidal gold. *Discuss. Faraday Soc.* **1951**, *11*, 55–75.

[42] Millstone, J. E.; Park, S.; Shuford, K. L.; Qin, L. D.; Schatz, G. C.; Mirkin, C. A. Observation of a quadrupole plasmon mode for a colloidal solution of gold nanoprisms. *J. Am. Chem. Soc.* **2005**, *127*, 5312–5313.

[43] Chen, L.; Ji, F.; Xu, Y.; He, L.; Mi, Y. F.; Bao, F.; Sun, B. Q.; Zhang, X. H.; Zhang, Q. High-yield seedless synthesis of triangular gold nanoplates through oxidative etching. *Nano Lett.* **2014**, *14*, 7201–7206.

[44] O'Brien, M. N.; Jones, M. R.; Brown, K. A.; Mirkin, C. A. Universal noble metal nanoparticle seeds realized through iterative reductive growth and oxidative dissolution reactions. *J. Am. Chem. Soc.* **2014**, *136*, 7603–7606.

[45] Wang, Q.; Wang, Z. P.; Li, Z.; Xiao, J. Y.; Shan, H. Y.; Fang, Z. Y.; Qi, L. M. Controlled growth and shape-directed self-assembly of gold nanoarrows. *Sci. Adv.* **2017**, *3*, e1701183.

[46] Zhang, Q.; Ge, J. P.; Pham, T.; Goebl, J.; Hu, Y. X.; Lu, Z. D.; Yin, Y. D. Reconstruction of silver nanoplates by UV irradiation: Tailored optical properties and enhanced stability. *Angew. Chem., Int. Ed.* **2009**, *48*, 3516–3519.

[47] Sun, Y. G.; Xia, Y. N. Shape-controlled synthesis of gold and silver nanoparticles. *Science* **2002**, *298*, 2176–2179.

[48] Zhang, Q.; Li, W. Y.; Moran, C.; Zeng, J.; Chen, J. Y.; Wen, L. P.; Xia, Y. N. Seed-mediated synthesis of Ag nanocubes with controllable edge lengths in the range of 30-200 nm and comparison of their optical properties. *J. Am. Chem. Soc.* **2010**, *132*, 11372–11378.

[49] Wu, J. J. X.; Tan, L. H.; Hwang, K.; Xing, H.; Wu, P. W.; Li, W.; Lu, Y. DNA sequence-dependent morphological evolution of silver nanoparticles and their optical and hybridization properties. *J. Am. Chem. Soc.* **2014**, *136*, 15195–15202.

[50] Yoo, H. J.; Kim, N.; Lee, H.; Kim, D.; Ow, L. T. C.; Nam, H.; Kim, C.; Lee, S. Y.; Lee, K. Y.; Kim, D. et al. Bespoke metal nanoparticle synthesis at room temperature and discovery of chemical knowledge on nanoparticle growth via autonomous experimentations. *Adv. Funct. Mater.* **2024**, *34*, 2312561.

[51] Murray, C. B.; Norris, D. J.; Bawendi, M. G. Synthesis and characterization of nearly monodisperse CdE (E = sulfur, selenium, tellurium) semiconductor nanocrystallites. *J. Am. Chem. Soc.* **1993**, *115*, 8706–8715.

[52] Talapin, D. V.; Rogach, A. L.; Kornowski, A.; Haase, M.; Weller, H. Highly luminescent monodisperse CdSe and CdSe/ZnS nanocrystals synthesized in a hexadecylamine-trioctylphosphine oxide-trioctylphospine mixture. *Nano Lett.* **2001**, *1*, 207–211.

[53] Kim, T.; Kim, K. H.; Kim, S.; Choi, S. M.; Jang, H.; Seo, H. K.; Lee, H.; Chung, D. Y.; Jang, E. Efficient and stable blue quantum dot light-emitting diode. *Nature* **2020**, *586*, 385–389.

[54] Gupta, A.; Ondry, J. C.; Lin, K. L.; Chen, Y. H.; Hudson, M. H.; Chen, M.; Schaller, R. D.; Rossini, A. J.; Rabani, E.; Talapin, D. V. Composition-defined optical properties and the direct-to-indirect transition in core-shell $In_{1-x}Ga_xP$/ZnS colloidal quantum dots. *J. Am. Chem. Soc.* **2023**, *145*, 16429–16448.

[55] Liu, L. P.; Zhuang, Z. B.; Xie, T.; Wang, Y. G.; Li, J.; Peng, Q.; Li, Y. D. Shape control of CdSe nanocrystals with zinc blende structure. *J. Am. Chem. Soc.* **2009**, *131*, 16423–16429.

[56] Fedin, I.; Talapin, D. V. Colloidal CdSe quantum rings. *J. Am. Chem. Soc.* **2016**, *138*, 9771–9774.

[57] Wang, L.; Li, W. T.; Yin, L. Q.; Liu, Y. J.; Guo, H. Z.; Lai, J. W.; Han, Y.; Li, G.; Li, M.; Zhang, J. H. et al. Full-color fluorescent carbon quantum dots. *Sci. Adv.* **2020**, *6*, eabb6772.

[58] Li, Y. J.; Tian, R. Z.; Shi, H. L.; Xu, J. Y.; Wang, T. T.; Liu, J. Q. Protein assembly: Controllable design strategies and applications in biology. *Aggregate* **2023**, *4*, e317.

[59] Kim, J.; Lee, S.; Kim, Y.; Choi, M.; Lee, I.; Kim, E.; Yoon, C. G.; Pu, K. Y.; Kang, H. E. M.; Kim, J. S. *In situ* self-assembly for cancer therapy and imaging. *Nat. Rev. Mater.* **2023**, *8*, 710–725.

[60] Bai, Y. S.; Luo, Q.; Liu, J. Q. Protein self-assembly via supramolecular strategies. *Chem. Soc. Rev.* **2016**, *45*, 2756–2767.

[61] Stephanopoulos, N. Hybrid nanostructures from the self-assembly of proteins and DNA. *Chem* **2020**, *6*, 364–405.

[62] Kamada, A.; Rodriguez-Garcia, M.; Ruggeri, F. S.; Shen, Y.; Levin, A.; Knowles, T. P. J. Controlled self-assembly of plant proteins into high-performance multifunctional nanostructured films. *Nat. Commun.* **2021**, *12*, 3529.

[63] Yang, G.; Ding, H. M.; Kochovski, Z.; Hu, R. T.; Lu, Y.; Ma, Y. Q.; Chen, G. S.; Jiang, M. Highly ordered self-assembly of native proteins into 1D, 2D, and 3D structures modulated by the tether length of assembly-inducing ligands. *Angew. Chem., Int. Ed.* **2017**, *56*, 10691–10695.

[64] Shapiro, D. M.; Mandava, G.; Yalcin, S. E.; Arranz-Gibert, P.; Dahl, P. J.; Shipps, C.; Gu, Y. Q.; Srikanth, V.; Salazar-Morales, A. I.; O'Brien, J. P. et al. Protein nanowires with tunable functionality and programmable self-assembly using sequence-controlled synthesis. *Nat. Commun.* **2022**, *13*, 829.

[65] Lapenta, F.; Aupič, J.; Vezzoli, M.; Strmšek, Ž.; Da Vela, S.; Svergun, D. I.; Carazo, J. M.; Melero, R.; Jerala, R. Self-assembly and regulation of protein cages from pre-organised coiled-coil modules. *Nat. Commun.* **2021**, *12*, 939.

[66] Snoj, J.; Lapenta, F.; Jerala, R. Preorganized cyclic modules facilitate the self-assembly of protein nanostructures. *Chem. Sci.* **2024**, *15*, 3673–3686.

[67] Watson, J. D.; Crick, F. H. C. Molecular structure of nucleic acids: A structure for deoxyribose nucleic acid. *Nature* **1953**, *171*, 737–738.

[68] Tang, Y.; Liu, H.; Wang, Q.; Qi, X. D.; Yu, L.; Šulc, P.; Zhang, F.; Yan, H.; Jiang, S. X. DNA origami tessellations. *J. Am. Chem. Soc.* **2023**, *145*, 13858–13868.

[69] Ji, W.; Xiong, X. W.; Cao, M. Y.; Zhu, Y.; Li, L.; Wang, F.; Fan, C. H.; Pei, H. Encoding signal propagation on topology-programmed DNA origami. *Nat. Chem.* **2024**, *16*, 1408–1417.

[70] Seeman, N. C. Nanotechnology and the Double Helix. *Sci. Am.* **2004**, *290*, 64–75.

[71] Seeman, N. C. Nucleic acid junctions and lattices. *J. Theor. Biol.* **1982**, *99*, 237–247.

[72] Kallenbach, N. R.; Ma, R. I.; Seeman, N. C. An immobile nucleic acid junction constructed from oligonucleotides. *Nature* **1983**, *305*, 829–831.

[73] Ma, R. I.; Kallenbach, N. R.; Sheardy, R. D.; Petrillo, M. L.; Seeman, N. C. Three-arm nucleic acid junctions are flexible. *Nucleic Acids Res.* **1986**, *14*, 9745–9753.

[74] Wang, X.; Seeman, N. C. Assembly and characterization of 8-Arm and 12-Arm DNA branched junctions. *J. Am. Chem. Soc.* **2007**, *129*, 8169–8176.

[75] Yan, H.; Park, S. H.; Finkelstein, G.; Reif, J. H.; LaBean, T. H. DNA-templated self-assembly of protein arrays and highly conductive nanowires. *Science* **2003**, *301*, 1882–1884.

[76] He, Y.; Tian, Y.; Chen, Y.; Deng, Z. X.; Ribbe, A. E.; Mao, C. D. Sequence symmetry as a tool for designing DNA nanostructures. *Angew. Chem., Int. Ed.* **2005**, *44*, 6694–6696.

[77] He, Y.; Chen, Y.; Liu, H. P.; Ribbe, A. E.; Mao, C. D. Self-assembly of hexagonal DNA two-dimensional (2D) arrays. *J. Am. Chem. Soc.* **2005**, *127*, 12202–12203.

[78] He, Y.; Tian, Y.; Ribbe, A. E.; Mao, C. D. Highly connected two-dimensional crystals of DNA six-point-stars. *J. Am. Chem. Soc.* **2006**, *128*, 15978–15979.

[79] Huang, K.; Yang, D. L.; Tan, Z. Y.; Chen, S. L.; Xiang, Y.; Mi, Y. L.; Mao, C. D.; Wei, B. Self-assembly of wireframe DNA nanostructures from junction motifs. *Angew. Chem., Int. Ed.* **2019**, *58*, 12123–12127.

[80] Yang, Q.; Chang, X.; Lee, J. Y.; Saji, M.; Zhang, F. DNA T-shaped crossover tiles for 2D tessellation and nanoring reconfiguration. *Nat. Commun.* **2023**, *14*, 7675.

[81] Rothemund, P. W. K. Folding DNA to create nanoscale shapes and patterns. *Nature* **2006**, *440*, 297–302.

[82] Douglas, S. M.; Dietz, H.; Liedl, T.; Högberg, B.; Graf, F.; Shih, W. M. Self-assembly of DNA into nanoscale three-dimensional shapes. *Nature* **2009**, *459*, 414–418.

[83] Dietz, H.; Douglas, S. M.; Shih, W. M. Folding DNA into twisted and curved nanoscale shapes. *Science* **2009**, *325*, 725–730.

[84] Han, D. R.; Pal, S.; Nangreave, J.; Deng, Z. T.; Liu, Y.; Yan, H. DNA origami with complex curvatures in three-dimensional space. *Science* **2011**, *332*, 342–346.

[85] Benson, E.; Mohammed, A.; Gardell, J.; Masich, S.; Czeizler, E.; Orponen, P.; Högberg, B. DNA rendering of polyhedral meshes at the nanoscale. *Nature* **2015**, *523*, 441–444.

[86] Jun, H.; Shepherd, T. R.; Zhang, K. M.; Bricker, W. P.; Li, S. S.; Chiu, W.; Bathe, M. Automated sequence design of 3D polyhedral wireframe DNA origami with honeycomb edges. *ACS Nano* **2019**, *13*, 2083–2093.

[87] Veneziano, R.; Ratanalert, S.; Zhang, K. M.; Zhang, F.; Yan, H.; Chiu, W.; Bathe, M. Designer nanoscale DNA assemblies programmed from the top down. *Science* **2016**, *352*, 1534.

[88] Pfeifer, W. G.; Huang, C. M.; Poirier, M. G.; Arya, G.; Castro, C. E. Versatile computer-aided design of free-form DNA nanostructures and assemblies. *Sci. Adv.* **2023**, *9*, eadi0697.

[89] Zhuang, J. M.; Garzoni, M.; Torres, D. A.; Poe, A.; Pavan, G. M.; Thayumanavan, S. Programmable nanoassemblies from non-assembling homopolymers using Ad Hoc electrostatic interactions. *Angew. Chem., Int. Ed.* **2017**, *56*, 4145–4149.

[90] Kalsin, A. M.; Fialkowski, M.; Paszewski, M.; Smoukov, S. K.;

Bishop, K. J. M.; Grzybowski, B. A. Electrostatic self-assembly of binary nanoparticle crystals with a diamond-like lattice. *Science* **2006**, *312*, 420–424.

[91] Fan, Q. S.; Li, Z. W.; Li, Y. C.; Gao, A. Q.; Zhao, Y. Z.; Yang, D.; Zhu, C. H.; Brinzari, T. V.; Xu, G. F.; Pan, L. et al. Unveiling enhanced electrostatic repulsion in silica nanosphere assembly: Formation dynamics of body-centered-cubic colloidal crystals. *J. Am. Chem. Soc.* **2023**, *145*, 28191–28203.

[92] Bian, T.; Gardin, A.; Gemen, J.; Houben, L.; Perego, C.; Lee, B.; Elad, N.; Chu, Z. L.; Pavan, G. M.; Klajn, R. Electrostatic co-assembly of nanoparticles with oppositely charged small molecules into static and dynamic superstructures. *Nat. Chem.* **2021**, *13*, 940–949.

[93] Gerling, T.; Wagenbauer, K. F.; Neuner, A. M.; Dietz, H. Dynamic DNA devices and assemblies formed by shape-complementary, non-base pairing 3D components. *Science* **2015**, *347*, 1446–1452.

[94] Wagenbauer, K. F.; Sigl, C.; Dietz, H. Gigadalton-scale shape-programmable DNA assemblies. *Nature* **2017**, *552*, 78–83.

[95] Thrasher, C. J.; Jia, F.; Yee, D. W.; Kubiak, J. M.; Wang, Y. P.; Lee, M. S.; Onoda, M.; Hart, A. J.; Macfarlane, R. J. Rationally designing the supramolecular interfaces of nanoparticle superlattices with multivalent polymers. *J. Am. Chem. Soc.* **2024**, *146*, 11532–11541.

[96] Li, J. H.; Fan, Y. R.; Gu, Q. X.; Zhou, X. Y.; Sun, H.; Du, J. Z. Homopolymer self-assembly: Principles, driving forces, and applications. *Chem. Mater.* **2023**, *35*, 10348–10370.

[97] Song, J. Y.; Ju, Y.; Amarasena, T. H.; Lin, Z. X.; Mettu, S.; Zhou, J. J.; Rahim, M. A.; Ang, C. S.; Cortez-Jugo, C.; Kent, S. J. et al. Influence of poly(ethylene glycol) molecular architecture on particle assembly and *ex vivo* particle-immune cell interactions in human blood. *ACS Nano* **2021**, *15*, 10025–10038.

[98] Chen, J. Q.; Pan, S. J.; Zhou, J. J.; Lin, Z. X.; Qu, Y. J.; Glab, A.; Han, Y. Y.; Richardson, J. J.; Caruso, F. Assembly of bioactive nanoparticles via metal-phenolic complexation. *Adv. Mater.* **2022**, *34*, 2108624.

[99] Sun, S. H.; Anders, S.; Hamann, H. F.; Thiele, J. U.; Baglin, J. E. E.; Thomson, T.; Fullerton, E. E.; Murray, C. B.; Terris, B. D. Polymer mediated self-assembly of magnetic nanoparticles. *J. Am. Chem. Soc.* **2002**, *124*, 2884–2885.

[100] Abul Kashem, M. M.; Patra, D.; Perlich, J.; Rothkirch, A.; Buffet, A.; Roth, S. V.; Rotello, V. M.; Müller-Buschbaum, P. Two- and three-dimensional network of nanoparticles via polymer-mediated self-assembly. *ACS Macro Lett.* **2012**, *1*, 396–399.

[101] Santos, P. J.; Gabrys, P. A.; Zornberg, L. Z.; Lee, M. S.; Macfarlane, R. J. Macroscopic materials assembled from nanoparticle superlattices. *Nature* **2021**, *591*, 586–591.

[102] Iinuma, R.; Ke, Y. G.; Jungmann, R.; Schlichthaerle, T.; Woehrstein, J. B.; Yin, P. Polyhedra self-assembled from DNA tripods and characterized with 3D DNA-PAINT. *Science* **2014**, *344*, 65–69.

[103] Liu, L. F.; Li, Z.; Li, Y. L.; Mao, C. D. Rational design and self-assembly of two-dimensional, dodecagonal DNA quasicrystals. *J. Am. Chem. Soc.* **2019**, *141*, 4248–4251.

[104] Wang, T. Q.; Bai, T. X.; Tan, Z. Y.; Ohayon, Y. P.; Sha, R. J.; Vecchioni, S.; Seeman, N. C.; Wei, B. Mesojunction-based design paradigm of structural DNA nanotechnology. *J. Am. Chem. Soc.* **2023**, *145*, 2455–2460.

[105] He, Y.; Ye, T.; Su, M.; Zhang, C.; Ribbe, A. E.; Jiang, W.; Mao, C. D. Hierarchical self-assembly of DNA into symmetric supramolecular polyhedra. *Nature* **2008**, *452*, 198–201.

[106] Wang, P. F.; Wu, S. Y.; Tian, C.; Yu, G. M.; Jiang, W.; Wang, G. S.; Mao, C. D. Retrosynthetic analysis-guided breaking tile symmetry for the assembly of complex DNA nanostructures. *J. Am. Chem. Soc.* **2016**, *138*, 13579–13585.

[107] Zheng, J. P.; Birktoft, J. J.; Chen, Y.; Wang, T.; Sha, R. J.; Constantinou, P. E.; Ginell, S. L.; Mao, C. D.; Seeman, N. C. From molecular to macroscopic via the rational design of a self-assembled 3D DNA crystal. *Nature* **2009**, *461*, 74–77.

[108] Simmons, C. R.; Buchberger, A.; Henry, S. J. W.; Novacek, A.; Fahmi, N. E.; MacCulloch, T.; Stephanopoulos, N.; Yan, H. Site-specific arrangement and structure determination of minor groove binding molecules in self-assembled three-dimensional DNA crystals. *J. Am. Chem. Soc.* **2023**, *145*, 26075–26085.

[109] Ma, N. N.; Dai, L. Z.; Chen, Z.; Ji, M.; Wang, Y.; Tian, Y. Environment-resistant DNA origami crystals bridged by rigid DNA rods with adjustable unit cells. *Nano Lett.* **2021**, *21*, 3581–3587.

[110] Ke, Y. G.; Ong, L. L.; Shih, W. M.; Yin, P. Three-dimensional structures self-assembled from DNA bricks. *Science* **2012**, *338*, 1177–1183.

[111] Ong, L. L.; Hanikel, N.; Yaghi, O. K.; Grun, C.; Strauss, M. T.; Bron, P.; Lai-Kee-Him, J.; Schueder, F.; Wang, B.; Wang, P. F. et al. Programmable self-assembly of three-dimensional nanostructures from 10,000 unique components. *Nature* **2017**, *552*, 72–77.

[112] Jones, M. R.; Macfarlane, R. J.; Lee, B.; Zhang, J.; Young, K. L.; Senesi, A. J.; Mirkin, C. A. DNA-nanoparticle superlattices formed from anisotropic building blocks. *Nat. Mater.* **2010**, *9*, 913–917.

[113] Zhang, C.; Macfarlane, R. J.; Young, K. L.; Choi, C. H. J.; Hao, L. L.; Auyeung, E.; Liu, G. L.; Zhou, X. Z.; Mirkin, C. A. A general approach to DNA-programmable atom equivalents. *Nat. Mater.* **2013**, *12*, 741–746.

[114] Lin, H. X.; Lee, S.; Sun, L.; Spellings, M.; Engel, M.; Glotzer, S. C.; Mirkin, C. A. Clathrate colloidal crystals. *Science* **2017**, *355*, 931–935.

[115] Park, S. S.; Urbach, Z. J.; Brisbois, C. A.; Parker, K. A.; Partridge, B. E.; Oh, T.; Dravid, V. P.; Olvera de la Cruz, M.; Mirkin, C. A. DNA- and field-mediated assembly of magnetic nanoparticles into high-aspect ratio crystals. *Adv. Mater.* **2020**, *32*, 1906626.

[116] Zhou, W. J.; Li, Y. W.; Je, K.; Vo, T.; Lin, H. X.; Partridge, B. E.; Huang, Z. Y.; Glotzer, S. C.; Mirkin, C. A. Space-tiled colloidal crystals from DNA-forced shape-complementary polyhedra pairing. *Science* **2024**, *383*, 312–319.

[117] Mirkin, C. A.; Letsinger, R. L.; Mucic, R. C.; Storhoff, J. J. A DNA-based method for rationally assembling nanoparticles into macroscopic materials. *Nature* **1996**, *382*, 607–609.

[118] Nykypanchuk, D.; Maye, M. M.; van der Lelie, D.; Gang, O. DNA-guided crystallization of colloidal nanoparticles. *Nature* **2008**, *451*, 549–552.

[119] Park, S. Y.; Lytton-Jean, A. K. R.; Lee, B.; Weigand, S.; Schatz, G. C.; Mirkin, C. A. DNA-programmable nanoparticle crystallization. *Nature* **2008**, *451*, 553–556.

[120] Hill, H. D.; Macfarlane, R. J.; Senesi, A. J.; Lee, B.; Park, S. Y.; Mirkin, C. A. Controlling the lattice parameters of gold nanoparticle FCC crystals with duplex DNA linkers. *Nano Lett.* **2008**, *8*, 2341–2344.

[121] Lin, Q. Y.; Mason, J. A.; Li, Z. Y.; Zhou, W. J.; O'Brien, M. N.; Brown, K. A.; Jones, M. R.; Butun, S.; Lee, B.; Dravid, V. P. et al. Building superlattices from individual nanoparticles via template-confined DNA-mediated assembly. *Science* **2018**, *359*, 669–672.

[122] Li, Y. W.; Zhou, W. J.; Tanriover, I.; Hadibrata, W.; Partridge, B. E.; Lin, H. X.; Hu, X. B.; Lee, B.; Liu, J. F.; Dravid, V. P. et al. Open-channel metal particle superlattices. *Nature* **2022**, *611*, 695–701.

[123] Zhou, W. J.; Lim, Y.; Lin, H. X.; Lee, S.; Li, Y. W.; Huang, Z. Y.; Du, J. S.; Lee, B.; Wang, S. Z.; Sánchez-Iglesias, A. et al. Colloidal quasicrystals engineered with DNA. *Nat. Mater.* **2024**, *23*, 424–428.

[124] Maye, M. M.; Kumara, M. T.; Nykypanchuk, D.; Sherman, W. B.; Gang, O. Switching binary states of nanoparticle superlattices and dimer clusters by DNA strands. *Nat. Nanotechnol.* **2010**, *5*, 116–120.

[125] Macfarlane, R. J.; Jones, M. R.; Lee, B.; Auyeung, E.; Mirkin, C. A. Topotactic interconversion of nanoparticle superlattices. *Science* **2013**, *341*, 1222–1225.

[126] Zhu, J. H.; Kim, Y.; Lin, H. X.; Wang, S. Z.; Mirkin, C. A. pH-responsive nanoparticle superlattices with tunable DNA bonds. *J. Am. Chem. Soc.* **2018**, *140*, 5061–5064.

[127] Lan, X.; Chen, Z.; Dai, G. L.; Lu, X. X.; Ni, W. H.; Wang, Q. B.

Bifacial DNA origami-directed discrete, three-dimensional, anisotropic plasmonic nanoarchitectures with tailored optical chirality. *J. Am. Chem. Soc.* **2013**, *135*, 11441–11444.
[128] Schreiber, R.; Do, J.; Roller, E. M.; Zhang, T.; Schüller, V. J.; Nickels, P. C.; Feldmann, J.; Liedl, T. Hierarchical assembly of metal nanoparticles, quantum dots and organic dyes using DNA origami scaffolds. *Nat. Nanotechnol.* **2014**, *9*, 74–78.
[129] Schreiber, R.; Santiago, I.; Ardavan, A.; Turberfield, A. J. Ordering gold nanoparticles with DNA origami nanoflowers. *ACS Nano* **2016**, *10*, 7303–7306.
[130] Wang, P. F.; Gaitanaros, S.; Lee, S.; Bathe, M.; Shih, W. M.; Ke, Y. G. Programming self-assembly of DNA origami honeycomb two-dimensional lattices and plasmonic metamaterials. *J. Am. Chem. Soc.* **2016**, *138*, 7733–7740.
[131] Ji, M.; Ma, N. N.; Tian, Y. 3D lattice engineering of nanoparticles by DNA shells . *Small* **2019**, *15*, 1805401.
[132] Xin, X. D.; Wang, L. H.; Wang, K. W.; Dai, L. Z.; Cao, H.; Li, Z.; Tian, Y. Stepwise assembly of nanoclusters guided by DNA origami frames with high-throughput. *Chem. Commun.* **2020**, *56*, 4918–4921.
[133] Xie, X. L.; Ji, M.; Yan, X. H.; Yu, Y. F.; Wang, Y.; Ma, N. N.; Xing, H.; Tian, Y. Layer-controllable "2.5D" DNA origami crystals synthesized by a hierarchical assembly strategy. *Angew. Chem., Int. Ed.* **2024**, *63*, e202402312.
[134] Martens, K.; Funck, T.; Santiago, E. Y.; Govorov, A. O.; Burger, S.; Liedl, T. Onset of chirality in plasmonic meta-molecules and dielectric coupling. *ACS Nano* **2022**, *16*, 16143–16149.
[135] Shen, C.; Lan, X.; Zhu, C.; Zhang, W.; Wang, L.; Wang, Q. Spiral patterning of Au nanoparticles on Au nanorod surface to form chiral AuNR@AuNP helical superstructures templated by DNA origami. *Adv. Mater.* **2017**, *29*, 1606533.
[136] Benn, F.; Haley, N. E. C.; Lucas, A. E.; Silvester, E.; Helmi, S.; Schreiber, R.; Bath, J.; Turberfield, A. J. Chiral DNA Origami nanotubes with well-defined and addressable inside and outside surfaces. *Angew. Chem., Int. Ed.* **2018**, *57*, 7687–7690.
[137] Heck, C.; Kanehira, Y.; Kneipp, J.; Bald, I. Placement of single proteins within the SERS hot spots of self-assembled silver nanolenses. *Angew. Chem., Int. Ed.* **2018**, *57*, 7444–7447.
[138] Pal, S.; Deng, Z. T.; Wang, H. N.; Zou, S. L.; Liu, Y.; Yan, H. DNA directed self-assembly of anisotropic plasmonic nanostructures. *J. Am. Chem. Soc.* **2011**, *133*, 17606–17609.
[139] Li, Y.; Pei, J.; Lu, X. H.; Jiao, Y. F.; Liu, F. S.; Wu, X. H.; Liu, J. B.; Ding, B. Q. Hierarchical assembly of super-DNA origami based on a flexible and covalent-bound branched DNA structure. *J. Am. Chem. Soc.* **2021**, *143*, 19893–19900.
[140] Kuzyk, A.; Schreiber, R.; Zhang, H.; Govorov, A. O.; Liedl, T.; Liu, N. Reconfigurable 3D plasmonic metamolecules. *Nat. Mater.* **2014**, *13*, 862–866.
[141] Zhou, C.; Duan, X. Y.; Liu, N. A plasmonic nanorod that walks on DNA origami. *Nat. Commun.* **2015**, *6*, 8102.
[142] Lan, X.; Liu, T. J.; Wang, Z. M.; Govorov, A. O.; Yan, H.; Liu, Y. DNA-guided plasmonic helix with switchable chirality. *J. Am. Chem. Soc.* **2018**, *140*, 11763–11770.
[143] Liu, W. Y.; Halverson, J.; Tian, Y.; Tkachenko, A. V.; Gang, O. Self-organized architectures from assorted DNA-framed nanoparticles. *Nat. Chem.* **2016**, *8*, 867–873.
[144] Dong, Y. X.; Liu, J. L.; Lu, X. Z.; Duan, J. L.; Zhou, L. Q.; Dai, L. Z.; Ji, M.; Ma, N. N.; Wang, Y.; Wang, P. et al. Two-stage assembly of nanoparticle superlattices with multiscale organization. *Nano Lett.* **2022**, *22*, 3809–3817.
[145] Michelson, A.; Minevich, B.; Emamy, H.; Huang, X. J.; Chu, Y. S.; Yan, H. F.; Gang, O. Three-dimensional visualization of nanoparticle lattices and multimaterial frameworks. *Science* **2022**, *376*, 203–207.
[146] Dai, L. Z.; Hu, X. X.; Ji, M.; Ma, N. N.; Xing, H.; Zhu, J. J.; Min, Q. H.; Tian, Y. Programming the morphology of DNA origami crystals by magnesium ion strength. *Proc. Natl. Acad. Sci. USA* **2023**, *120*, e2302142120.
[147] Tian, Y.; Zhang, Y. G.; Wang, T.; Xin, H. L.; Li, H. L.; Gang, O. Lattice engineering through nanoparticle-DNA frameworks. *Nat. Mater.* **2016**, *15*, 654–661.
[148] Liu, W. Y.; Tagawa, M.; Xin, H. L.; Wang, T.; Emamy, H.; Li, H. L.; Yager, K. G.; Starr, F. W.; Tkachenko, A. V.; Gang, O. Diamond family of nanoparticle superlattices. *Science* **2016**, *351*, 582–586.
[149] Tian, Y.; Lhermitte, J. R.; Bai, L.; Vo, T.; Xin, H. L.; Li, H. L.; Li, R. P.; Fukuto, M.; Yager, K. G.; Kahn, J. S. et al. Ordered three-dimensional nanomaterials using DNA-prescribed and valence-controlled material voxels. *Nat. Mater.* **2020**, *19*, 789–796.
[150] Ji, M.; Liu, J. L.; Dai, L. Z.; Wang, L.; Tian, Y. Programmable cocrystallization of DNA origami shapes. *J. Am. Chem. Soc.* **2020**, *142*, 21336–21343.
[151] Ji, M.; Zhou, Z. Y.; Cao, W. H.; Ma, N. N.; Xu, W. G.; Tian, Y. A universal way to enrich the nanoparticle lattices with polychrome DNA origami "homologs". *Sci. Adv.* **2022**, *8*, eadc9755.
[152] Huang, S. J.; Ji, M.; Wang, Y.; Tian, Y. Geometry guided crystallization of anisotropic DNA origami shapes. *Chem. Sci.* **2023**, *14*, 11507–11514.
[153] Coropceanu, I.; Janke, E. M.; Portner, J.; Haubold, D.; Nguyen, T. D.; Das, A.; Tanner, C. P. N.; Utterback, J. K.; Teitelbaum, S. W.; Hudson, M. H. et al. Self-assembly of nanocrystals into strongly electronically coupled all-inorganic supercrystals. *Science* **2022**, *375*, 1422–1426.
[154] Grabenhorst, L.; Sturzenegger, F.; Hasler, M.; Schuler, B.; Tinnefeld, P. Single-molecule FRET at 10 MHz count rates. *J. Am. Chem. Soc.* **2024**, *146*, 3539–3544.
[155] Haddadnezhad, M.; Jung, I.; Oh, M. J.; Park, S. Ready-to-use free-standing super-powder made with complex nanoparticles for SERS. *Adv. Mater.* **2024**, *36*, 2400068.
[156] Kuzyk, A.; Schreiber, R.; Fan, Z. Y.; Pardatscher, G.; Roller, E. M.; Högele, A.; Simmel, F. C.; Govorov, A. O.; Liedl, T. DNA-based self-assembly of chiral plasmonic nanostructures with tailored optical response. *Nature* **2012**, *483*, 311–314.
[157] Peil, A.; Zhan, P. F.; Duan, X. Y.; Krahne, R.; Garoli, D.; Liz-Marzán, L. M.; Liu, N. Transformable plasmonic helix with swinging gold nanoparticles. *Angew. Chem., Int. Ed.* **2023**, *62*, e202213992.
[158] Niu, R. J.; Song, C. Y.; Gao, F.; Fang, W. N.; Jiang, X. Y.; Ren, S. K.; Zhu, D.; Su, S.; Chao, J.; Chen, S. F. et al. DNA origami-based nanoprinting for the assembly of plasmonic nanostructures with single-molecule surface-enhanced Raman scattering. *Angew. Chem., Int. Ed.* **2021**, *60*, 11695–11701.
[159] Li, K.; Wang, K.; Qin, W. W.; Deng, S. H.; Li, D.; Shi, J. Y.; Huang, Q.; Fan, C. H. DNA-directed assembly of gold nanohalo for quantitative plasmonic imaging of single-particle catalysis. *J. Am. Chem. Soc.* **2015**, *137*, 4292–4295.
[160] Fu, J. J.; Zhu, W. L.; Chen, Y.; Yin, Z. Y.; Li, Y. Y.; Liu, J.; Zhang, H. Y.; Zhu, J. J.; Sun, S. H. Bipyridine-assisted assembly of Au nanoparticles on Cu nanowires to enhance the electrochemical reduction of CO_2. *Angew. Chem., Int. Ed.* **2019**, *58*, 14100–14103.
[161] Kumari, G.; Kamarudheen, R.; Zoethout, E.; Baldi, A. Photocatalytic surface restructuring in individual silver nanoparticles. *ACS Catal.* **2021**, *11*, 3478–3486.
[162] Zhang, F. H.; Liu, R. J.; Wei, Y. Z.; Wei, J. J.; Yang, Z. J. Self-assembled open porous nanoparticle superstructures. *J. Am. Chem. Soc.* **2021**, *143*, 11662–11669.
[163] Auyeung, E.; Morris, W.; Mondloch, J. E.; Hupp, J. T.; Farha, O. K.; Mirkin, C. A. Controlling structure and porosity in catalytic nanoparticle superlattices with DNA. *J. Am. Chem. Soc.* **2015**, *137*, 1658–1662.
[164] Wang, S. Z.; Park, S. S.; Buru, C. T.; Lin, H. X.; Chen, P. C.; Roth, E. W.; Farha, O. K.; Mirkin, C. A. Colloidal crystal engineering with metal-organic framework nanoparticles and DNA. *Nat. Commun.* **2020**, *11*, 2495.

[165] Zhang, D.; Chen, Y. D.; Hao, M.; Xia, Y. N. Putting hybrid nanomaterials to work for biomedical applications. *Angew. Chem., Int. Ed.* **2024**, *63*, e202319567.
[166] Levin, A.; Hakala, T. A.; Schnaider, L.; Bernardes, G. J. L.; Gazit, E.; Knowles, T. P. J. Biomimetic peptide self-assembly for functional materials. *Nat. Rev. Chem.* **2020**, *4*, 615–634.
[167] Egwu, C. O.; Aloke, C.; Onwe, K. T.; Umoke, C. I.; Nwafor, J.; Eyo, R. A.; Chukwu, J. A.; Ufebe, G. O.; Ladokun, J.; Audu, D. T. et al. Nanomaterials in drug delivery: Strengths and opportunities in medicine. *Molecules* **2024**, *29*, 2584.
[168] Qi, G. B.; Gao, Y. J.; Wang, L.; Wang, H. Self-assembled peptide-based nanomaterials for biomedical imaging and therapy. *Adv. Mater.* **2018**, *30*, 1703444.
[169] Zhang, W. Q.; Zeng, Y. H.; Xiao, Q. Q.; Wu, Y. Y.; Liu, J. L.; Wang, H. C.; Luo, Y. T.; Zhan, J.; Liao, N.; Cai, Y. B. An *in-situ* peptide-antibody self-assembly to block CD47 and CD24 signaling enhances macrophage-mediated phagocytosis and anti-tumor immune responses. *Nat. Commun.* **2024**, *15*, 5670.
[170] Rahman, M. M.; Wang, J.; Wang, G. S.; Su, Z. P.; Li, Y. Z.; Chen, Y. D.; Meng, J. G.; Yao, Y.; Wang, L. F.; Wilkens, S. et al. Chimeric nanobody-decorated liposomes by self-assembly. *Nat. Nanotechnol.* **2024**, *19*, 818–824.
[171] Saccà, B.; Niemeyer, C. M. DNA origami: The art of folding DNA. *Angew. Chem., Int. Ed.* **2012**, *51*, 58–66.
[172] Li, Y. G.; Cu, Y. T. H.; Luo, D. Multiplexed detection of pathogen DNA with DNA-based fluorescence nanobarcodes. *Nat. Biotechnol.* **2005**, *23*, 885–889.
[173] Bandy, T. J.; Brewer, A.; Burns, J. R.; Marth, G.; Nguyen, T.; Stulz, E. DNA as supramolecular scaffold for functional molecules: Progress in DNA nanotechnology. *Chem. Soc. Rev.* **2011**, *40*, 138–148.
[174] Li, S. P.; Jiang, Q.; Liu, S. L.; Zhang, Y. L.; Tian, Y. H.; Song, C.; Wang, J.; Zou, Y. G.; Anderson, G. J.; Han, J. Y. et al. A DNA nanorobot functions as a cancer therapeutic in response to a molecular trigger *in vivo*. *Nat. Biotechnol.* **2018**, *36*, 258–264.
[175] Hu, X. X.; Chi, H. L.; Fu, X. Y.; Chen, J. L.; Dong, L. Y.; Jiang, S. Q.; Li, Y.; Chen, J. Y.; Cheng, M.; Min, Q. H. et al. Tunable multivalent aptamer-based DNA nanostructures to regulate multiheteroreceptor-mediated tumor recognition. *J. Am. Chem. Soc.* **2024**, *146*, 2514–2523.